Master's thesis

NTNU
Norwegian University of Science and Technology
Faculty of Natural Sciences
Department of Biology

Nalia Hama

Using a low-cost high throughput microscope in cultivated seaweed farms for early biofouling detection

Master's thesis in Ocean Resources
Supervisor: Glaucia Moreira Fragoso (IBI)
Co-supervisor: Ana Borrero (Seaweed Solutions AS) and Yngvar Olsen (IBI)

May 2024

NTNU
Norwegian University of Science and Technology

Nalia Hama

Using a low-cost high throughput microscope in cultivated seaweed farms for early biofouling detection

Master's thesis in Ocean Resources
Supervisor: Glaucia Moreira Fragoso (IBI)
Co-supervisor: Ana Borrero (Seaweed Solutions AS) and Yngvar Olsen (IBI)
May 2024

Norwegian University of Science and Technology
Faculty of Natural Sciences
Department of Biology

NTNU
Norwegian University of
Science and Technology

Abstract

Fouling of bryozoan colonies is one of the major challenges for the seaweed industry in Mid and South Norway. *Membranipora membranacea* and *Electra pilosa* are two prominent bryozoan species that lead to biofouling on seaweed in temperate waters. The biofouling makes the flexible kelp lamina brittle and susceptible to breakage, and thus loss of valuable biomass for the producers. The encrusting fouling also reduces the value of the product by making it unsuitable for human food consumption.

There is a need for developing specialized instruments on bryozoan larval detection and size estimation in the water column, as this could be an important tool to detect the timing of settlement on cultivated kelp. The aim of this study was to investigate the use of a home-built flow through microscope (AFTI-scope) as a potential semi-automated method to quantify abundance estimates, and to monitor larval size changes of *E. pilosa* and *M. membranacea.* The relationship between the timing of the bloom, the abundance and size of bryozoan larvae (cyphonautes) and the timing of settlement on the kelp was investigated. This was to verify whether larval size and concentration changes over time could be used as a tool for early biofouling detection. The overall abundance of *M. membranacea* and *E. pilosa* larvae in the water was analyzed during the sea cultivation period from February to June 2023 at two stations in Frøya, Trøndelag – one by the edge of a kelp farm and another half km apart.

The AFTI-scope underestimated larval counts by an average of 26 % compared to the traditional microscope method. For *E. pilosa* the two methods yielded statistically different abundance estimates. For *M. membranacea* the method showed no significant difference in the estimates, proving suitable detection capabilities for this species with the current AFTI-scope settings. The size of the cyphonautes reached their biggest size in late May and beginning of June. This was followed by two peaks in settled bryozoan larvae observed on *Saccharina latissima*, one in May and one in June. The increase in larvae of different size observed over time, suggested growth, and possibly different stages of development. This was potentially linked to environmental conditions such as temperature, which showed a positive correlation with larval size. No correlation was found between bryozoan size and chlorophyll concentrations, suggesting that existing phytoplankton levels were sufficient for bryozoan growth.

The first peak in cyphonaute abundance was observed after the spring bloom (April). The second peak (June) occurred after the first signs of settlement of larvae on the kelp. This could suggest a round of new populations of larvae from the recent settled colonies. No signs of correlation with increasing temperatures and abundance for neither of the species was observed. However, settlement did not occur as larval abundance reached its first peak. This might be due to the cyphonautes not being mature at that point. The findings underscore the importance of considering larval size, rather than only abundance, in their ability to settle on the kelp lamina. AFTI-scope has the potential for further development, where the size dependent settlement of cyphonaute on *S. latissima* could be a proxy for early fouling detection.

Sammendrag

Begroing på kultivert tare som følge av mosdyrkolonier er en av hovedutfordringene for tareindustrien i Midt- og Sør-Norge. *Membranipora membranacea* og *Electra pilosa* er to fremtredende mosdyrarter som fører til begroing på tare i temperert sjø. Begroing gjør det fleksible tarebladet skjørt, slik at det lettere brekker av, og fører til tap av verdifull biomasse for tareprodusentene. Den skorpedannende begroingen reduserer også verdien av produktet ved å gjøre det uegnet for menneskelig konsum.

Som følge av dette er det behov for å utvikle metoder for påvisning av mosdyrlarver i vannmassene rundt tareanlegg. Abundansen av mosdyrlarver og deres størrelse kan indikere tidspunktet mosdyrlarver fester seg på dyrket tare. Målet med denne studien var å undersøke bruken av et hjemmesnekret gjennomstrømningsmikroskop (AFTI-scope) som en potensiell semi-automatisert metode for å kvantifisere abundansen av mosdyrlarver, samt overvåke endringer i larvestørrelse for *M. membranacea* og *E. pilosa.* Forholdet mellom våroppblomstring, abundans og larvestørrelse ved tidspunkt for kolonidannelse ble undersøkt. Dette ble gjort for å undersøke om data for abundans og larvestørrelse over tid kan brukes for tidlig påvisning av begroing. Abundansen av *M. membranacea* og *E. pilosa* ble estimert i dyrkningsperioden i sjø fra februar til juni 2023 ved to stasjoner på Frøya, en ved kanten av et tareanlegg (MI) og en 0,5 km unna (MO).

AFTI-skopet underestimerte i snitt 26 % lavere abundans sammenlignet med et lysmikroskop. For *E. Pilosa* gav de to metodene statistisk forskjellige abundansestimat, mens for *M. membranacea* viste metoden ingen signifikant forskjell i estimatene, noe som indikerte gode deteksjonsevner for denne arten med det aktuelle AFTI-scopet. Mosdyrlarvene var størst i slutten av mai og begynnelsen av juni. Det var også da de to høyeste konsentrasjonene med mosdyrlarver var festet på Saccharina latissima. Variasjonen i larvestørrelse blant individer ble observert over tid. Det indikerte vekst og muligens ulike utviklingsstadier, potensielt knyttet til miljøforhold som temperatur, som viste en positiv korrelasjon med larvestørrelse. Det ble ikke funnet noen sammenheng mellom larvestørrelse og klorofyllkonsentrasjoner, noe som tyder på at eksisterende fytoplanktonnivåer var tilstrekkelige for vekst av mosdyrlarvene.

Den første økningen i planktoniske larver ble observert etter våroppblosmtringen (april). Den andre tydelige økningen i abundans skjedde i juni, i etterkant av de første tegnene på begroing av larver på taren. Dette tydet på nye populasjoner av larver spredt fra de bosatte koloniene. Ingen tegn til korrelasjon med økende temperaturer og abundans ble observert for noen av artene. Begroingen skjedde imidlertid ikke da mengden larver nådde sin første topp. Dette kan skyldes at larvene ikke var modne på dette tidspunktet. Resultatene understreker viktigheten av larvestørrelse i tillegg til abundansestimeringer for deres evne til å sette seg på taren. AFTI-scope har potensialet for videre forskning på størrelsesavhengig begroing av mosdyrlarver på *S. lattisima*.

Acknowledgements

This MSc project has been completed at the Norwegian University of Science and Technology in the period from December 2022 to May 2024. This thesis was part of the following project: "Autonomous underwater monitoring of kelp-farm biomass, growth, health and biofouling using optical sensors", MoniTARE (315514) (2021-2025) and funded by the Research Council of Norway (RCN). Access to the kelp farm in Frøya was provided by Seaweed Solutions. Labwork was conducted at Trondheim Biologen Station.

Firstly, I want to thank my supervisor Glaucia Moreira Fragoso for letting me join this exciting project. It has been an enriching process, and I am grateful for all the support and feedback along the way. Secondly, I want to thank my co-supervisors, Ana Borrero for providing feedback on results and writing, and Yngvar Olsen for insightful guidance and helpful feedback, especially in the last stages. I also want to thank Siv Anina Etter for all the analysis, and for making TBS a great place for everyone. To Dag Altin and Rune Bjørgum for saving my project with great technical support, and Mathias Haugum for always being available whenever I needed technical assistance with the AFTI-scope. To Maja Karoline Viddal Hatlebakk for doing all the taxonomic counts and for taking the time to answer all my questions.

I would also like to thank all the people at SES for the cooperation and help during field work. A special thanks to the KELPie team - Els and Adrian for making all the long field days memorable. I am glad I got to share this with you.

As this thesis marks the completion of my time as a student in Trondheim it cannot come to an end without thanking the people who have made these last five years some of the best ones of my life. To Hedda and Marie, thank you for making Trondheim feel more like home since my first year in town. I will forever cherish our friendship. To my fellow students at Njord, thank you for all the memories and fun times we have shared. I want to thank my fellow board members of Njord for sharing some of my greatest times as a student with me. A special thanks to the girls at TBS: Anja, Ingeborg, Els, Maria, Hedda and Birgitte for making the absolute best environment to be in while finishing our most stressful work. Having you girls to lean one has made even the toughest day, the days I will remember the most.

Lastly, I want to thank the people closest to my heart for always supporting me. I am truly blessed to be surrounded by or only a phone call away. You make me realize the important things in life, and for that I will always be grateful. To my parents and sisters whom never fail at making me feel loved – خۆشم دەوێن هەمیشە. هەمیشە سوپاسگوزارتانم، بۆ ئەو دەرفەتانەی پێتان بەخشیم.

Trondheim, May 2024

Nalia Hama

Table of Contents

List of Abbreviations

Chl a	Chlorophyll *a*
CTD	Conductivity, Temperature, and Depth
EtOH	Ethanol
FChl a	Chlorophyll *a* fluorescence
FOV	Field of view
FTU	Formazine Turbidity Unit
HABs	Harmful Algal Blooms
MI	Inside the kelp farm
MO	Outside the kelp farm
NCC	Norwegian Coastal Current
NOK	Norwegian krone
OPC	Optical Plankton Recorder
RPM	Revolutions per minute
R&D	Research and development
SES	Seaweed Solutions
TBS	Trondheim Biological Station

1 Introduction

1.1 Seaweed aquaculture

As the global population expands, the need for sustainable food sources intensifies. The oceans, rich in potential for biomass production, could significantly contribute to meeting this need. Seaweed cultivation stands out as a viable strategy to ensure sustainable food security in the future (FAO, 2022).

Seaweed aquaculture is rapidly growing, and the production volumes have tripled in the last 20 years (World Bank, 2023). On a global scale, the aquaculture production reached 122.6 million tonnes in 2020. Aquatic algae accounted for 35.1 million tonnes wet weight according to the FAO Fisheries and Aquaculture Department's statistics (2022).

Currently, global seaweed production is dominated by a small number of East and Southeast Asian nations, where modern seaweed farming became established in the 1950s to 1970s (Hwang et al., 2019). According to a report published by the World Bank (2023) Asian producers dominate the market in both volume and value, with more than 98 % of market share. China and Indonesia are the two greatest seaweed producers and supply 56 % and 27 % of the farmed seaweed volume, respectively. In 2020, only 2 % of the total volume of cultivated seaweed was farmed outside Asia (World Bank, 2023).

The use of seaweed includes a wide range of bioactive products of potentially high market value (Holdt & Kraan, 2011). The applications of seaweed include human food, animal feed products, fertilizers, prebiotics, cosmetics, bioactive peptides and pharmaceuticals and nutraceuticals (Charrier et al., 2017; Fernand et al., 2017; van den Burg et al., 2016). Despite of this, seaweed is a relatively underexploited resource in Europe that has gained a growing interest in aquaculture business in recent decades due to a growing market demand (Buschmann et al., 2017; van den Burg et al., 2016), as well as obtaining environmental and societal benefits (Kraan, 2020). For seaweed cultivation, there is no need for input factors such as feed, fertilizers, or freshwater (Padam & Chye, 2020). Seaweed farming also contributes to lower the atmospheric levels of carbon dioxide by fixating inorganic carbon as a primary producer (Krause-Jensen & Duarte, 2016). Additionally, cultivation of seaweed can mitigate ocean acidification and eutrophication by taking up excess nutrients in eutrophic waters (Duarte et al., 2017; Lange et al., 2020).

Enhancing seaweed production and optimizing value chains can contribute to meeting at least nine of the 17 U.N. Sustainable Development Goals (World Bank, 2023).

1.2 Seaweed aquaculture in Norway

Seaweed and its market products are predicted to play an important role in the emerging Norwegian bioeconomy. Some point towards scenarios where the Norwegian seaweed aquaculture industry has the potential to produce 20 million tonnes by 2050 (Broch et al., 2019; Olafsen et al., 2012; Skjermo et al., 2014).

In Norway seaweed cultivation is a developing industry, and only became established in Europe in the last 5-10 years (Zhang et al., 2022). The first commercial permits for cultivation of seaweeds in Norway were granted in 2014 (Stévant et al., 2017). Since then, permits for both monoculture cultivation of seaweeds and in Integrated multitrophic aquaculture (IMTA) systems have increased from 54 to 522 in 2023 (Fiskeridirektoratet, 2022b). Norway is characterized as a highly suitable region for seaweed aquaculture due to the long coastline, making it suitable for establishing sites for cultivation (Stévant et al., 2017). It also has a favorable climate with nutrient-rich inflow of Atlantic water (Sætre, 2007). Norway is also among the world-leading nations in marine aquaculture and offshore operations, combined with a strong tradition in marine research. There is no other country in Europe with as many seaweed aquaculture companies, making Norway the top producer of seaweed biomass in Europe in volume (Araújo et al., 2021). A total of 25 companies were producing seaweed for commercial use in 2022 (Fiskeridirektoratet, 2022c).

In spite of great potential, large-scale seaweed production in Norway is not meeting the demands of the market. This is partly due to the market requirements for a big amount of predictable delivery of high-quality seaweed biomass. The industry is still facing challenges related to efficient farm monitoring, mitigation of biofouling growth and intensive workload (Skjermo et al., 2014), as well as biomass handling and processing after harvest (Stévant & Rebours, 2021). The production has mainly focused on *Saccharina latissima.* Due to its high nutrient content, excellent growth and high biomass potential (Bojorges et al., 2022), it is often destined for the food market and direct human consumption (Stévant et al., 2017). *Alaria esculenta* is the second most cultivated species in Norway. In 2022, 221 tonnes seaweed was produced in Norways. *S. latissima* accounted for 161 tonnes and *A. esculenta* accounted for 60 tonnes. All other species put together represented less than a ton produced the same year (Fiskeridirektoratet, 2022a).

In 2023, Norway's total seaweed production reached a value of NOK 4.227 million (Fiskeridirektoratet, 2022a). These numbers represent the quantity of harvested seaweed for human consumption and feed. The Norwegian Seaweed Association estimated the total production from seaweed farms to equal roughly 400 tonnes in 2023 (Albrecht, 2023). The gap between commercialized and overall harvest highlights that many seaweed producers are still in the developmental phase, and not necessarily commercially active even with ongoing production (Albrecht, 2023). Currently, the focus in Norway's seaweed sector is on expansion and up-scaling. Despite this, some experts (Campbell et al., 2021; Hadjimichael, 2018; Pauly, 2018) have questioned whether industry maturity necessarily requires large-scale industrialization. They raise the potential for growth in small-scale, locally based, sustainable practices (Campbell et al., 2021; Voyer et al., 2018), emphasizing the varied benefits of seaweed farming. The majority of Norwegian seaweed producers generate less than 50 tonnes annually, and economic viability hinges on up-scaling to offset high investment costs (Albrecht, 2023). Advancements in technology is essential to address production bottlenecks and support growth.

1.3 Biofouling on kelp

Biofouling is one of the main challenges and constrains in the development and expansion of the seaweed aquaculture industry (Bannister et al., 2019; Getachew et al., 2015; Lüning & Mortensen, 2015; Stévant et al., 2017). Biofouling is unwanted because it makes the seaweed more susceptible to breakage by making the frond stiff and crispy (Dixon et al., 1981). It is shown that *Saccharina longicruris* encrusted with *Membranipora membranacea* was more susceptible to breakage than non-encrusted specimens (Krumhansl et al., 2011). Several studies have shown how *M. membranacea* caused macroalgae lamina to become more fragile and easily break during bad weather conditions (Dixon et al., 1981; Pratt & Grason, 2007). The breakage of fronds leads to less biomass available for harvest by producers. In addition, the biofouling inhibits further growth of the cultivated kelp due to sunlight not penetrating the lamina and reaching the chlorophyll (Pratt & Grason, 2007). A study done in Skagerrak, Norway in natural beds of *S. latissima* concluded that heavy biofouling reduced access to light and thus disrupting the natural life cycle of the kelp (Andersen et al., 2011). Biofouling has also proven to yield less nutrient dense seaweed by creating a barrier to nutrient uptake (Hurd et al., 2000).

The cultivation of *S. latissima* in Trøndelag, has showed highest growth rates from February to June (Forbord et al., 2012). Fouling have been proved to settle in mid-June with continued increase during late June and July (Førde et al., 2016). The biofouling can lead to loss of biomass and necrosis in the distal end of the frown (Forbord et al., 2012). To avoid the unwanted effects of biofouling, it is suggested that, for the Trøndelag coast, *S. latissima* should be harvested from late April to early June at the latest (Førde et al., 2016).

1.4 Biology of bryozoans

M. membranacea and *Electra pilosa* are native bryozoan species that make up the dominant biofouling community for seaweed aquaculture in Norwegian waters (Førde et al., 2016; Pratt & Grason, 2007). Bryozoans have two life stages: either as sessile colonies encrusted on a surface, or as planktotrophic larvae, known as cyphonautes (Fuchs et al., 2011). Both *E. pilosa* and *M. membranacea* have an annual life cycle. As cyphonautes they are filter feeders that feed on phytoplankton and particles in the water column (Ryland & Stebbing, 1971). Cyphonautes of both species can be found year-round, *M. membranacea* cyphonautes are found to be especially abundant from May to September (Ryland, 1965). Cyphonautes of *M. membranacea* has been documented to have a basal edge of 840 µm and oral-aboral length of 640 µm when ready to settle before metamorphosis. The cyphonaut of *E. pilosa* is smaller in size and appear rather opaque without ornamentation along the basal edge. It is found to have a basal edge of 440 µm and oral aboral length of 360 µm when settling (Atkins, 1955).

Once settled, the larva undergoes metamorphosis and forms a single ancestrula zooid, that give rise to a colony by producing a series of identical zooids by asexually budding. *M. membranacea* larvae give raise to twin ancestrula zooids when settling (Atkins, 1955). The colonies are suspension feeders, and use a specialized organ consistent of ciliated tentacle that directs the food particles towards the mouth by generating their own feeding current (Winston et al., 1977). *M. membranacea* may remain in the plankton for weeks or months before settling on a substrate (Ryland & Stebbing, 1971). This is due to metamorphic competence, which is a crucial developmental stage that allows larvae of many aquatic invertebrates to swim and feed in the planktonic sphere while retaining the ability to settle and metamorphose in response to environmental cues (Zeng et al., 2022). Transformation

from a cyphonaut larva to a postlarval juvenile is promoted by the development of rudiments of juvenile structures within the larva (Hadfield, 2000; Hadfield et al., 2001).

Colonies of the two species can be distinguished based on the pattern they form on the lamina: *M. membranacea* colonies have a circular shape, whereas *E. pilosa* colonies are star-shaped (Figure 1). The walls that enclose each individual zooid are lightly calcified, and together they create highly organized colonies (Figure 1). The calcification makes the zooecia more flexible and thus more able to withstand bending of lamina it inhabits (Seed & O'Connor, 1981). The zooids produce gametes that occurs in the early spring and follows continuously during the early summer that give rise to cyphonautes (Ryland, 1965).

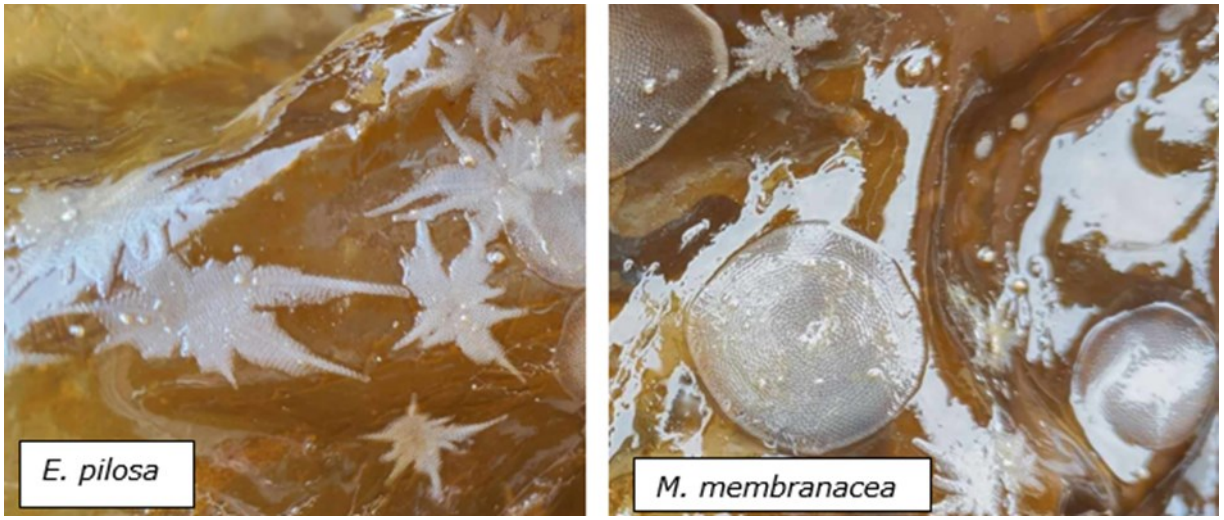

Figure 1: Colony shape of *Electra pilosa* and *Membranipora membranacea* on the kelp lamina. Photos with permission by Elisabeth Sniijder.

1.5 Monitoring of bryozoans – AFTI-scope

Technological innovation is needed to upscale the industry due to ineffective and labor-intensive methods that serve as bottlenecks in the production systems (Albrecht, 2023). A primary challenge is the development of cost-effective production techniques for monitoring, harvesting and processing of large volumes of seaweed, a prerequisite for reaching profitability (Kraan, 2020; Overrein et al., 2024). Although technologization requires a substantial investment, it can be a solution for the high labor costs in Norway and lead to increased operational efficiency (Albrecht, 2023). There is a pressing need for research and development (R&D) strategies that will enable upscaling of seaweed aquaculture to ultimately become a viable industry. A number of fields of R&D has been identified as prerequisites for an industry scale seaweed production, include biofouling control (Skjermo et al., 2014).

Establishing technologies which allow for data collection with little human input, are a straightforward step in providing a holistic, ecosystem-approach to monitoring the marine environment. Environmental DNA metabarcoding is a relatively new monitoring tool, that has been tested for accurate and cost-effective detection of species in environmental samples from Salmon aquaculture industry (Peters et al., 2018).

Monitoring of phytoplankton communities in fish farming has been used to detect harmful algal blooms (HABs) as these can produce toxins that pose serious human health risks

(Young et al., 2020). The development of high-throughput sequencing technology has helped to characterize the phytoplankton communities present in water (Burki et al., 2021). Jiang et al. (2020) found that the algal community structure in areas of macroalgae farming is more stable and the risk of HABs is low. This is due to the seaweeds ability to absorb a large amount of nutrients. Recent advances have also allowed the development of automated or semi-automated methods for zooplankton imaging (Lombard et al., 2019). The ZooScan (Naito et al., 2019) and FlowCam (Álvarez et al., 2013) are the two most prominent examples of imaging systems close to traditional microscopy.

The AFTI-scope is a new bench top tool, which is similar to other plankton imaging technologies, such as the ZooScan and FlowCam. Inspired by the novel PlanktoScope, which is a low-cost (< 500 €) flow through microscope (Pollina et al., 2022), it was developed by Haugum (2022) for high throughput imagining of plankton. The motivation was to develop a flow-through particle imaging system for cost effective and automated plankton sampling. The design is based on a light microscope, connected to a pump and a camera. The pump moves seawater underneath a magnifying objective lens, and the camera then take pictures of the sample. A darkfield condenser offers an increased contrast over conventional brightfield lighting. The methodology is explained in Chapter 2. The ultimate ambition of the AFTI-scope is to integrate machine learning to automatically identify and count plankton taxa from the images. In this thesis, the AFTI-scope was used to assess its potential as a monitoring tool for bryozoan abundance at a seaweed farm.

1.6 Aim of study

This main objective of this present master thesis was to assess the use of the AFTI-scope, a flow-through particle imaging system as a method for efficient counting and image sampling of bryozoan larvae in seaweed farming facilities. With the collected data, provided information was further investigated to look at the interactions between the abiotic and biotic factors that affect bryozoan larval growth in the water column and settlement on the cultivated kelp species *S. latissima*.

To achieve this, three sub-objectives were established:

1. Quantify bryozoan larvae in water using the AFTI-scope and traditional microscope and compare the accuracy of the optical method (AFTI-scope).

2. Investigate the relationship between temperature and chlorophyll a concentration and bryozoan larval concentrations to see if settlement increases with high larval abundance of late developmental stages in the water.

3. Analyze the size of the bryozoan larvae from AFTI-images and assess whether settlement on kelp is size-dependent.

2 Materials and methods

2.1 Study site

The present study was conducted in a kelp farm in Frøya island (Figure 2), off the coast of Central Norway, Trøndelag (Figure 3). This kelp concession called Måsskjæra belongs to Seaweed Solutions (SES) (63°44.617'N 8°52.756'E). The fieldwork was done at two sites, one by the edge of the seaweed farm (station MI) and another outside (station MO), approximately 500 m from MI (Figure 3).

The area is known to be biologically productive with intensive fishing and aquaculture activities (Ervik et al., 2018; Jevne et al., 2021). The area is characterized by complex currents due to strong winds, shallow and uneven bathymetry, and water mixing events (from tides and storms). Two major currents is found in the coast of Norway - the North Atlantic Current, which is a warm and nutrient-rich waters that lies beneath the Norwegian Coastal Current (NCC), a relatively low salinity water mass (Sætre, 2007). The NCC is comprised by freshwater runoff from fjords (including Trondheimsfjord) that accumulates along the coast of Norway (Michelsen et al., 2019; Skagseth et al., 2011) particularly from spring to autumn. The seabed topography is comprised of mixed substrates, with large rock structures separated by areas with soft sediments (Keeley et al., 2019). The highly variable bathymetry creates a complex water dynamic.

Figure 2: Seaweed Solutions' kelp farm, where the fieldwork was conducted. Photo with permission from Seaweed Solutions.

Måsskjæra is a semi-exposed kelp farm with depth ranging from 8 to 35 m. The location is exposed to north-eastly winds and sheltered from westerly and southerly winds (Førde et al., 2016). The cultivation site is approximately 400 × 400 m and is based on a horizontal longline system divided into approximately 16 cultivation squares (Overrein et al., 2024)(Figure 3). The two main cultivated species at the cultivation site of SES are *S. latissima* (sugar kelp or European kombu) and *A. esculenta* (winged kelp or European wakame / Atlantic wakame).

Both species were seeded onto a 2 mm twine (polyester) at SES's hatchery in Trondheim. Seedlings were deployed with a size of 1.5 cm. The seeded lines were vectorized around a 15 m stretch of carrying rope of 14 mm diameter. The distances between each line were 1.5 m. The cultivation depth was around 3 m depth.

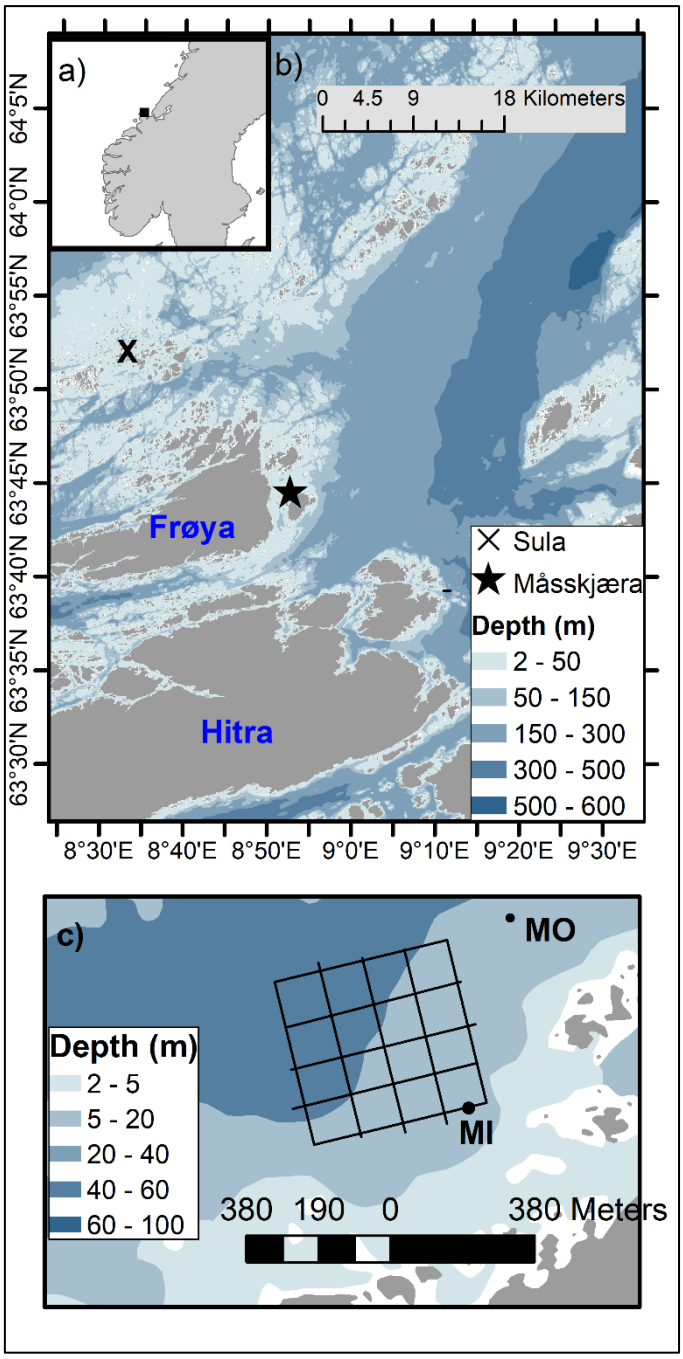

Figure 3: a) Map of the geographical location of Måsskjæra kelp farm located off the coast of central Norway. b) The location of the seaweed farm, including Sula meteorological station (star symbol), where wind data were retrieved. c) Illustrations of the layout of the seaweed farm and the sampling sites for environmental data and bryozoan larval abundance (Stations MI and MO).

2.2 Water and net sampling

Water and net sampling (more details below) were undertaken at both sites (Figure 3). Fieldwork occurred once to twice a month from February to June 2023, adding to nine sampling days in total. Selection of sampling days was partially dependent on weather and tidal conditions (preferably low tides and weak wind conditions for consistency), as well as personnel availability. However, due to the dynamic weather conditions of the study area and short time frame, not all sampling was done in consistent conditions, where in practice, it occurred with varying environmental conditions (Table 1).

Table 1: Date of field days (2023) and water sampling time. Water level conditions at Måsskjæra (kartverket.no), average wind speed (seklima.no) and wind direction (yr.no) measurements from closest meteorological station (Sula meteorological station, 10.4 km from Måsskjæra) at the time of sampling.

Field day	*Date*	*Time*	*Water level (cm)*	*Wind (m/s)*	*Wind Direction*
Day 1	February 15	8.00 - 10.00	164 – 125 (Ebbing)	5.15	SE
Day 2	March 16	8.30 – 11.00	131 – 89 (Ebbing)	8.47	SE
Day 3	March 29	9.00 – 11.00	117 – 89 (Ebbing)	5.8	SE
Day 4	April 18	8.15 – 10.00	133 – 194 (Rising)	1.45	SE SW
Day 5	April 25	8.50 – 11.00	63 – 64 (Low)	5.8	NE
Day 6	May 10	8.35 – 10.00	59 - 58 (Low)	2.6	SE/ WSW
Day 7	May 23	15.40 - 18.00	177 – 112 (Ebbing)	3.6	W SW
Day 8	June 7	8.40 – 12.30	30 – 166 (Rising)	7.4	SW
Day 9	June 29	8.30 – 12.30	190 – 106 (Ebbing)	3.18	NE SW

Seawater samples were collected with a custom-made 5 L water sampler, at 3 m depth at each site. The water was stored in two 8 L acid-washed dark bottles and later the same day filtered for nutrients and chlorophyll a (Chl a) *in vitro* analysis.

At the SES laboratory onshore, triplicate water samples were filtered (from 0.25L – 0.5L, depending on the phytoplankton concentration) through Glass Fiber Filters (Whatman 2.5 µm pore size, hydrophilic glass fiber filter, 25 mm diameter) with a vacuum pump. The filters were folded, then covered in aluminum foil and put in a zip lock plastic bag. They were immediately stored in dry ice for transportation and transferred to a -80°C freezer at Trondheim biological station (TBS), where it was kept until analysis of Chl a *in vitro*.

For nutrient concentrations (nitrate plus nitrite [NO_2^-+ NO_3^-]), hereafter referred to as nitrate [NO_3], and ammonium [NH_4], triplicate water samples from each station were filtered with a 0.8 µm polycarbonate filter, after being flushed to remove artificial ammonium in the filter. The filtrate (~ 45 ml of each sample) was placed into centrifuge tubes and kept at dry ice for transportation and stored at -20 °C in the freezer until further analysis.

Zooplankton net sampling was conducted for estimating bryozoan larval abundance. Vertical hauls (upper 5 m) were done using a handheld zooplankton net (100 µm mesh size and 40 cm in diameter) and a closed cod-end. Triplicate samples were collected at each station and sampling date. The net was rinsed with 96% ethanol (EtOH) each time and preserved in this solvent in 200 mL plastic bottles and stored in room temperature for later analysis.

Sampling of kelp specimens was also undertaken during the fieldwork. This was to detect when settlement of the larvae occurred on the kelp lamina and the bryozoan coverage throughout the season. The data and method used for estimating bryozoan coverage was developed during the same project. A more detailed methodology will be found in the master thesis of Elisabeth Alice Snijder, which is under preparation (Snijder, 2024).

2.3 Environmental data collection

Environmental data were further collected with sensors (details below) to investigate if, and to what extent, they affect bryozoan larval densities. To record the physical properties of the water column at each station, vertical profiles (down to 10 - 15 m) of conductivity, temperature turbidity and chlorophyll in response to density were performed at each station using a CTD device (model SD204 SAIV A/S™).

A C3 submersible fluorometer sensor (Turner Designs, USA) was located at 3 m depth and attached to the frame of the farm at station MI. The sensor collected time-series data of chlorophyll a fluorescence (FChl a, $mg.m^{-3}$), turbidity (FTU) and temperature (°C) every 10 minutes from 15th of February to 29th of June. FChl a re-emits light in the red spectrum when exposed to a blue LED from the submersible fluorometer sensor and, if interpreted carefully, it can serve as a proxy for FChl a concentration. In this study, it was used to determine the development and intensity of phytoplankton concentrations during the sampling period.

2.4 Laboratory analysis

For Chl a *in vitro* extractions the filters were removed from the -80°C freezer and individually placed in 15 ml glass tubes with 5 ml cold (~4 °C) 100% methanol (CH_3OH). The glass tubes were mixed gently using a vortex and placed in a freezer (-20 °C) for 24 h.

After extraction the filters were removed, and the solvent was filtered into new glass tubes. A syringe with 0.2 µm filter was used to remove contamination derived from the filter. About 5 ml of the solvent was pipetted into a small glass vial for analysis of the fluorescence. The fluorescence signals were measured using a Turner Design Fluorometer. The Chl a *in vitro* concentrations were calculated by using Equation 1.

Equation 1:

$$\text{Chl } a \text{ µg.L}^{-1} = \frac{(\mathbf{FL}-\mathbf{BL})*\mathbf{f}*\mathbf{E}*\mathbf{1000}}{\mathbf{V}*\mathbf{1000}}$$

Where FL is the fluorescence measured, BL is the blank sample (100% methanol), f is the calibration factor (0.47), E is the extraction volume (5 ml), and V is the filtered volume (45 ml).

2.4.1 Nutrient analysis

Filtered seawater samples for $[NO_3]$ and $[NH_4]$ were analyzed at TBS by a professional laboratory engineer. Analysis for $[NO_3]$ in water samples was done by using Flow Solution IV system O.I. Analytical Auto analyzer according to the Norwegian standard 4724 and 4745 respectively. Determination of $[NH_4]$ was done by direct segment flow analysis according to Kérouel and Aminot (1997).

2.5 Bryozoan larval abundance

Identification and quantification of *M. membranacea* and *E. pilosa* were performed at TBS by a taxonomist using a Leica (model M205C) dissecting microscope. The EtOH-preserved samples were drained over a 110 µm mesh and rinsed with EtOH. After rinsing, the samples were flushed into a plastic beaker for counting and diluted to a known volume. Subsamples of 3.5 mL were pipetted into a plexiglass counting chamber with four grooves, and the number of *M. membranacea* and *E. pilosa* larvae were counted. Subsamples were taken from each sample until 100 individuals of at least one of the species had been counted, or until the whole sample had been counted. Calculations were made to provide the taxa individual individuals per m^3 (number of bryozoans larvae in the total sample / total water sampled (0.628 m^3).

2.6 AFTI-scope for counting and imaging

2.6.1 AFTI-scope setup

The AFTI-scope is a flow through, open-source microscope developed by Haugum (2022) and designed to capture images of particles in water samples inspired by the PlanktoScope design (Pollina et al., 2022). The base component for the system is a BRESSER Science TFM-301 Trino microscope with a dosing pump connected (Figure 4). The pump is designed to transport the water sample from the inlet to a transparent Ibidi channel slide located below the microscope objective, allowing for objects of interest to be imaged.

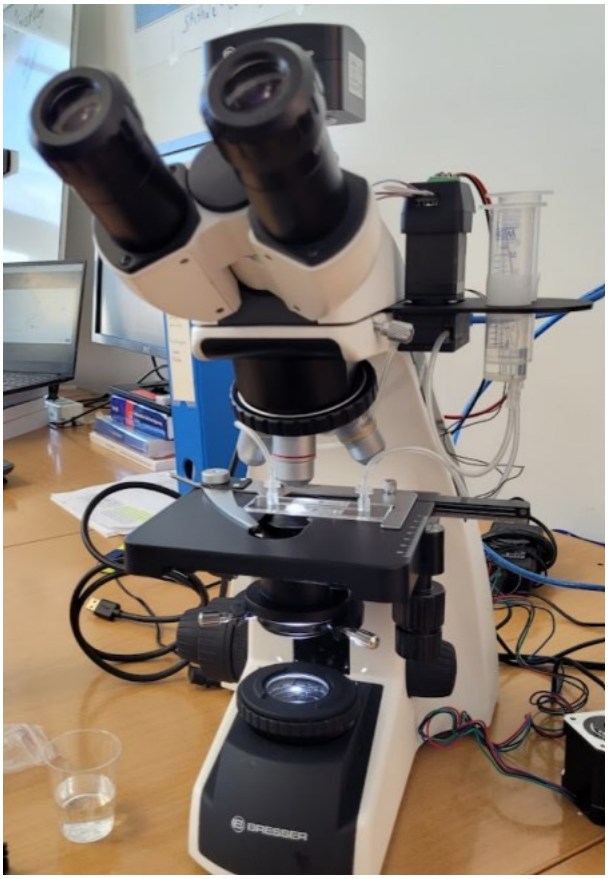

Figure 4: The AFTI-scope scope assembled on the Bresser Trino TFM-301 microscope. Photo with permission from Mathias Haugum.

Two 20 ml syringe barrels were fixed to the microscope with a three dimensional printed holder, serving as sample holders before and after the sample was pumped underneath the microscope objective. The samples were pumped from the inlet-syringe through flexible silicone tubing to the microscope channel slide. The slides were transparent, had a depth of 0.8 mm and attachment points for silicone tubing. The samples were led through the pump after the microscope slide, until it ended up in the outlet-syringe. The speed and direction of the pumped samples was controlled through a designated application programmed in Python (package PyQt5) on a Linux computer. The same program allowed for refocusing should the objective move (Figure 5).

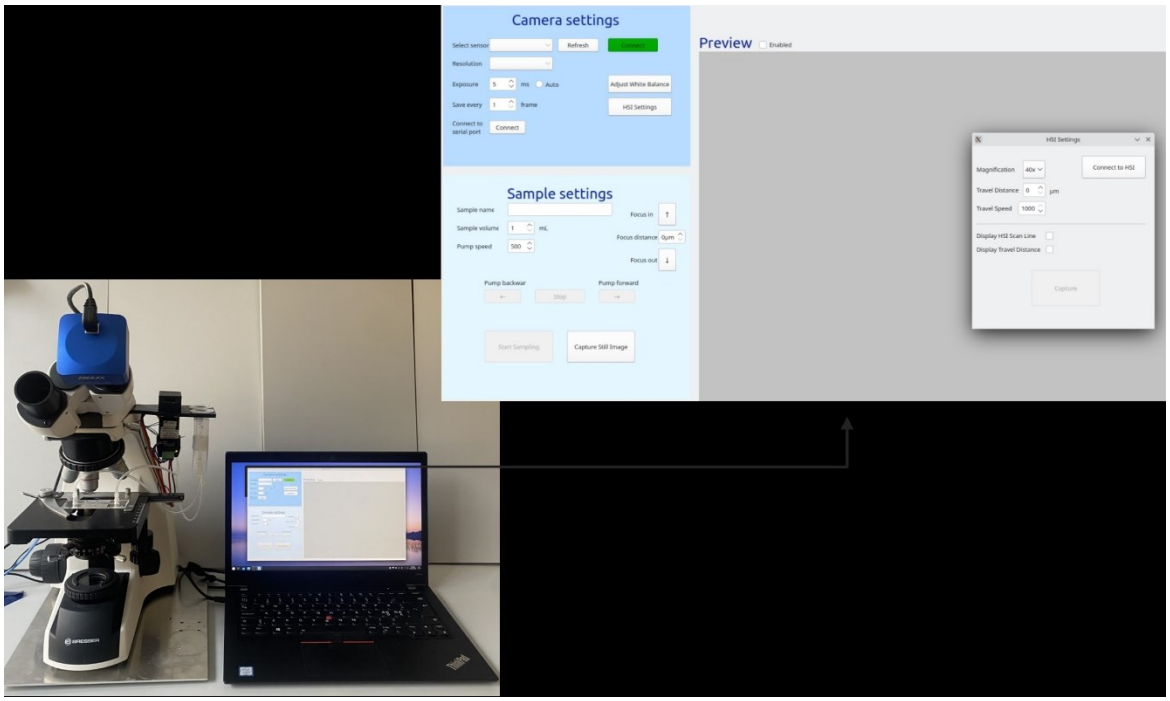

Figure 5: The setup at lab with the Linux computer that controlled the pump and settings. Camera and sample related settings are controlled and when the camera was connected, a preview was shown in the gray window (Haugum et al., 2023).

The inner tubing of the pump can be of different size and diameter, which affects the flow rate. In this setup, a tube with a diameter of 2 mm was used due to image the size range of bryozoan larvae. This allowed for flow rates up to 60 $ml.min^{-1}$. However, this was when the pump speed was set to maximum speed of 2000 revolutions per minute (rpm). On average the pump was set somewhere between 20 – 300 rpm depending on the subsample (Table 2). The flow rate varied between 0.6 $ml.min^{-1}$ at minimum and 9.1 $ml.min^{-1}$ at maximum.

Using microscope channel slides (µ-Slide I Luer, Ibidi) with a width of 5 mm and a depth of 0.8 mm, the ratio between the field of view (FOV) width and the channel width was found to be ≈ 0.46. The imaged volume was, thus, less than the actual pumped volume due to the FOV being reduced and approximately half of the slide was seen, therefore, adjustments had to be done to estimate the total number of bryozoan larval concentration in each sample (Equation 2).

Equation 2

$$Y = \text{Total number of individuals per sample} * 2.5$$

The camera was attached to the top ocular using the C-mount threads and connected to a PC using a USB3.0 cable. The pump driver was connected to the CNC shield and power supply as shown in Figure 6 (Haugum, 2022). With a 1.23MP camera recording at a magnification of 100x and image size of 1280x960 pixels, a resolution of 0.82 µm/pixel was achieved.

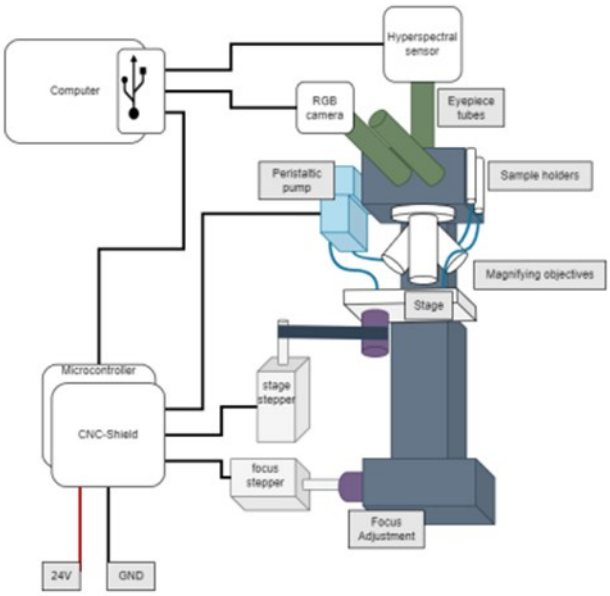

Figure 6: Schematic drawing made by Mathias Haugum of the connections and parts in the system. The microcontroller and cameras are connected to the computer using USB-cables, while the pump receives power and step signals from the CNC-shield (Haugum et al., 2023).

2.6.2 Laboratory protocol

In this thesis the AFTI-scope was used for quantification and size estimation of bryozoan larvae.

For that, a total of 21 net samples from station MI were pumped through the AFTI-scope. The reason for this was lack of time to analyze both station MI and MO. Triplicate net samples from 16th of March to 7th of June were analyzed (Table 2). Analyzing samples from February to early June gave the opportunity to compare how the AFTI-scope handled samples with varying abundances of plankton and organic material. This would also detect if the system was optimal for all samples or if an "ideal" sample was needed for the method to work.

All samples inserted in the AFTI-scope were first handled by a taxonomist for manual counting, and then tested with the AFTI-scope. The manual counting of bryozoans using a dissecting microscope was used for validation and as a threshold for the accuracy of the samples counted in the AFTI-scope.

Table 2: Sampling days from station MI analysed in the AFTI-scope.

Field day	**March 16th**	**March 29th**	**April 18th**	**April 25th**	**May 10th**	**May 23rd**	**June 7th**
Pump speed (rpm)	20-40	40	40-300	40 -300	20	20	20
Subsample	#1 #2 #3	#1 #2 #3	#1 #2 #3	#1 #2 #3	#1 #2 #3	#1 #2 #3	#1 #2 #3

The net samples were placed over a 130 µm mesh to drain out the EtOH. After drained, the samples were rinsed into a plastic beaker with EtOH, and the final volumes were noted down. The organic matter left in the mesh was scrapped from the mesh, placed into a Petri dish and examined under a Leica dissecting microscope (model M205C) to make sure all bryozoan larvae were rinsed, and none was left in the mesh. If any bryozoan larvae were detected in the Petri dish, they were manually counted (Figure 7) to make sure the estimations of larval abundance per sample was accurate. The net sample, in EtOH, was then placed in the inlet- syringe and run through the AFTI-scope. The speed of the pump was adjusted according to the concentration of particles in the sample in order to keep a flow that enabled the camera to capture images of the larvae in the channel slide. When the material from the net sample got clogged in the tube near the microscopic channel slide, the tube was manually removed, and the clogged material was put into a petri dish for further examination under the dissecting microscope. If bryozoan larvae were detected in the petri dish, they were re-pumped through the AFTI-scope so the camera could register their presence. The whole net sample was analyzed for all of the samples.

Figure 7: Schematic drawing of the laboratory protocol before samples were pumped through the AFTI-scope.

The number of bryozoan larvae individuals was noted in real time as the samples were pumped through the AFTI-scope. Calculations were made to provide the total taxa individuals per sample by multiplying the total number of individuals in each sample to the FOV (0.46). Then, to get the total individuals per number m^3, the total water volume (V) from each net haul was estimated according to Equation 3:

Equation 3:

$$\boldsymbol{V = \pi * r^2 * h}$$

Where π (3.14) is a constant, r is the radius (20 cm) of the net and h is the depth by which the net was dragged (5 m).

For each larvae observed, pictures were taken and identified as *M. membranacea* or *E. pilosa*. In cases of uncertainty of the identification, an expert taxonomist reclassified the pictures if needed.

2.6.3 Image Processing

To investigate the trends in bryozoan larval size as a function of time (from February to June), manual annotation of length and width were performed using the image processing program ImageJ. The pipeline started with sorting the images that included bryozoan larvae by the sampling day and uploading them in ImageJ. Then, using the "line" tool in ImageJ, two lines were manually drawn on each larvae picture: one representing the antero-posterior basal axis (basal edge) and another one from oral to aboral axis (length) (Figure 8). An image of a microscopic ruler taken with the AFTI-scope in the same setup was used as size reference to set a scale of pixels per centimeter (pixels.cm^{-1}) for the corresponding frame.

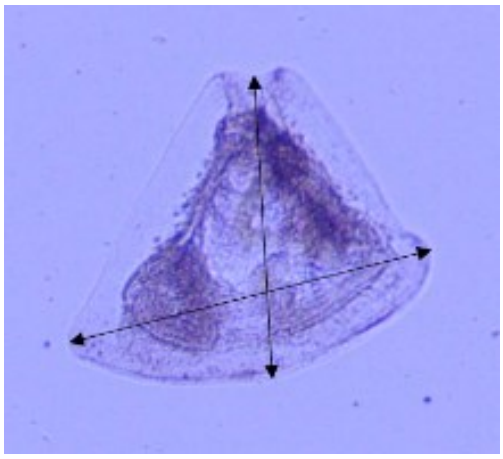

Figure 8: Lines showing the size measurements (basel edge and length) extracted from each bryozoan larva individual – antero-posterior basal axis (basel edge, horizontal line) and oral-aboral axis (length, vertical line).

2.7 Statistical analysis

All statistical analysis and graphs were conducted in R (version 4.3.3) through RStudio™ (version 2023.12.1). All data were tested for normality using a Shapiro-Wilk test. A non-parametric Mann-Whitney U-test was used to derive the statistical differences between stations for abundance of *E. pilosa* and *M. membranacea*. The same test was also used for deriving the statistical differences between the nutrient concentrations at both stations, as well as the statistical difference between the AFTI-scope and traditional microscopic counts.

The package Ggplot in R was used to make the graphs including the scatter plots of the CTD data, the time series of temperature, Chl a and turbidity, the NO_3 and NH_4 concentration at station MI and MO, the abundance of *E. pilosa* and *M. membranacea* at station MI and station MO, the box plots for maximum basal edge and oral-aboral length and the box plot comparing AFTI-scope versus microscopic counting.

Non-parametric, pair-wise Spearman correlation coefficients and statistical significance was calculated between environmental values, abundance, and size estimates of *E. pilosa* and *M. membranacea* using the corrplot package in R.

The significance limit for the analysis was set to 0.05. The values are presented with standard deviation (SD).

3 Results

3.1 Enviromental conditions

3.1.1 Vertical CTD profiles

CTD profiles for salinity and temperature (Figure 9) and Chl a and turbidity (Figure 10) are displayed to show the depth pattern at the different locations throughout the experimental period.

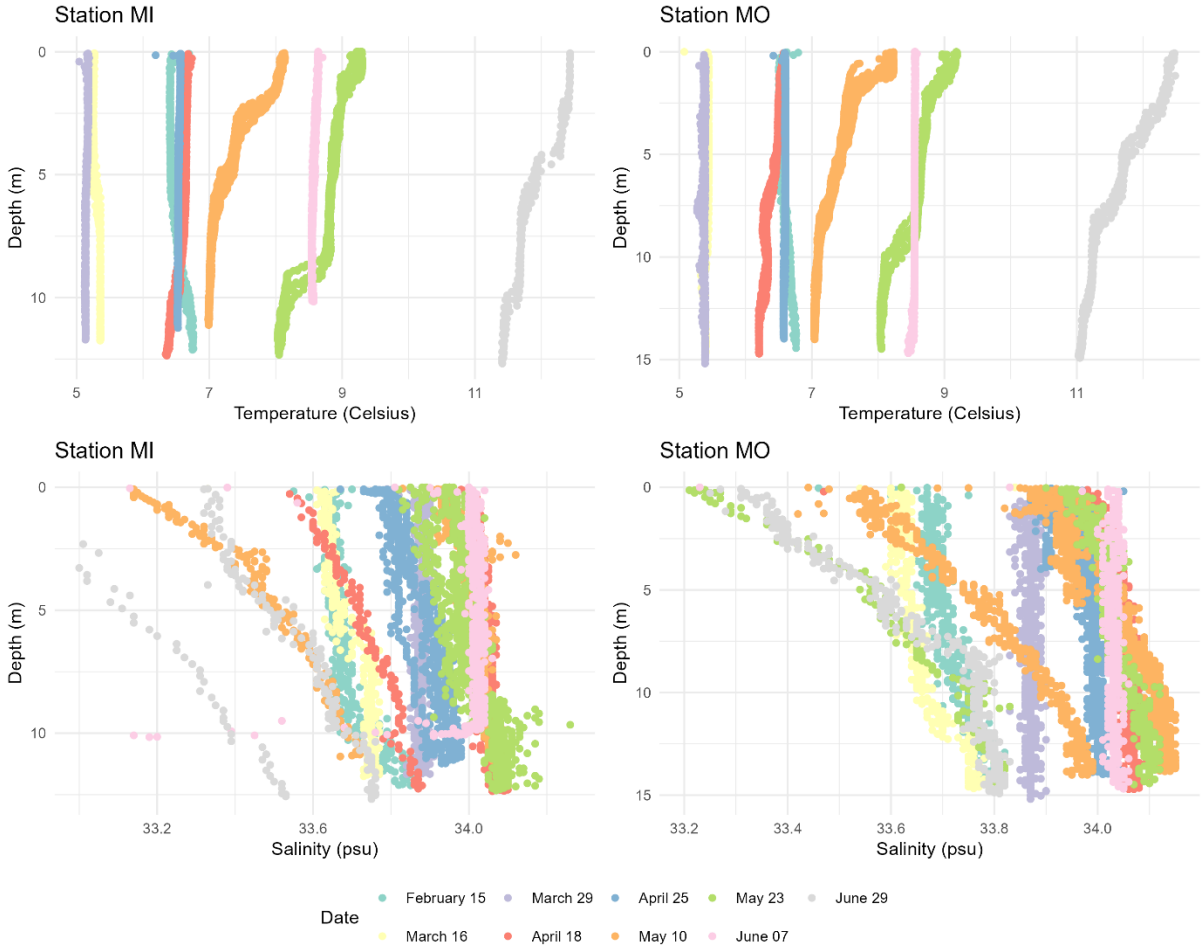

Figure 9: Vertical profiles of temperature and salinity at station MI (inside the farm-left) and MO (outside the kelp farm). Top row: temperature profiles (in Celsius) across sampling dates. Bottom Row: salinity profiles (practical salinity Units, psu) across sampling dates. Colors denote different measurement dates.

Temperature showed a clear trend of increasing temperatures from 5 °C in March to rising temperatures throughout the sampling period, reaching 12.5 °C in the end of June. Some stratification was observed in the deeper layers on the 25th of April. However, the water column was relatively well mixed until mid-May. The water had a pycnocline at

approximately 8 meters depth the 23rd of May. Stratification was broken down on the 7th of June and became stratified again the 29th of June (Figure 9).

Salinity ranged from 32.68 to 34.26, with a slight variation between the stations (Figure 9). The salinity showed lower values at the start of the sampling period, followed by a subsequent rise during the spring months, where it gradually remained stable before it dropped by the end of June. Stratification was shown May 10th and 23rd, and later the 29th of June (Figure 9).

Chl a concentrations were highest in the upper 12m of the most stratified waters (Figure 10). High concentrations of Chl a were also observed on 18th of April when the water column was not stratified. Chl a concentration increased from 18th of April (mean = 4.35 µg.L^{-1}, SD ± 4.99) and remained at a high concentration until it dropped again on 29th of June (mean = 1.68 µg.L^{-1}, SD ± 1.08).

Turbidity showed an increasing pattern with time, with values ranging from 0.01 to 250 Formazin Turbidity Unit (FTU) during the sampling period (Figure 10). Similar to Chl a, the water column showed high values of turbidity when the water column was stratified, on 10th (mean = 0.87 µg.L^{-1}, SD ± 3.02) and 23rd of May (mean = 0.79 µg.L^{-1}, SD ± 2.98).

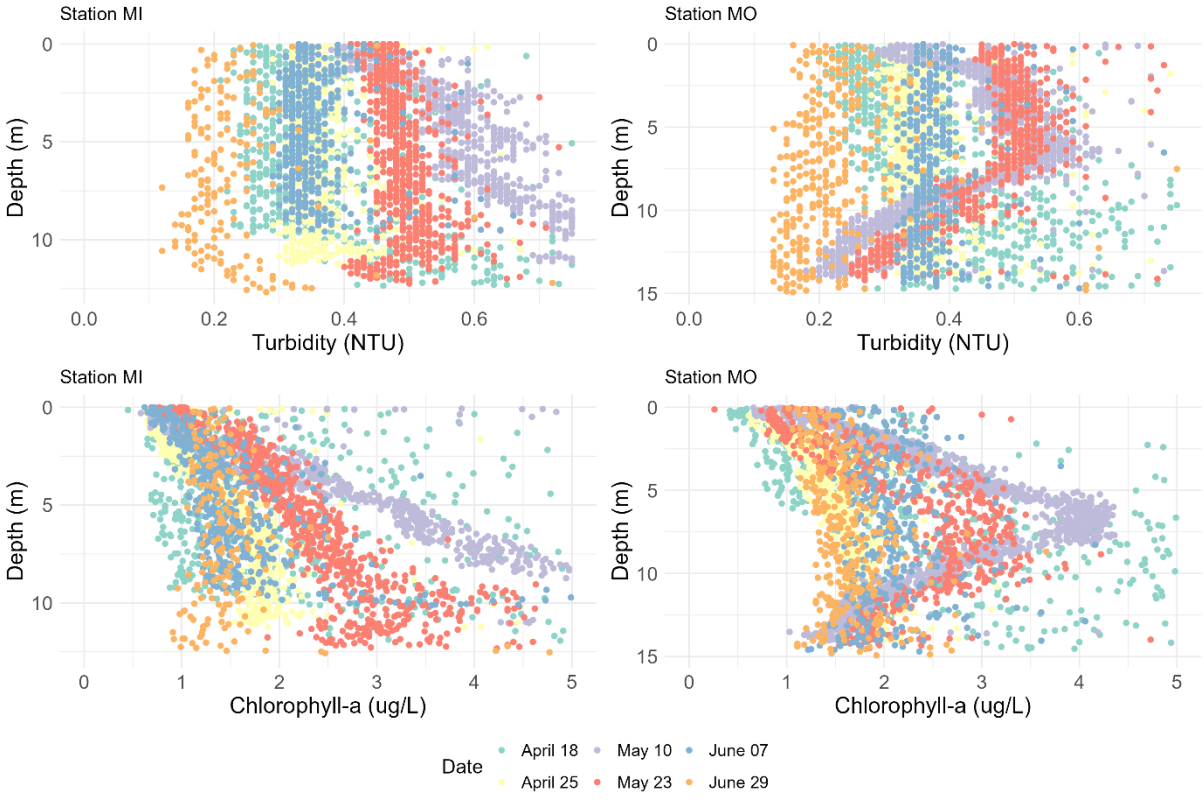

Figure 10: Vertical profiles of chlorophyll a (µg.L^{-1}) and turbidity (Formazin Turbidity Unit) at station MI (inside the farm) and MO (outside the kelp farm). Top row: temperature profiles (in Celsius) across sampling dates. Bottom Row: salinity profiles (practical salinity Units, psu) across sampling dates. Colors denote different measurement dates.

3.1.2 Time series measurements

Figure 11 shows temperature (°C), turbidity (FTU) and Chl *a* concentration (mg.m^{-3}) in the water as a time series from 15th of 29th of June.

Seawater temperature had a steady increase over the sampling period, varying from approximately 6 °C in mid-February to 12 °C in late June (Figure 11). The seawater temperatures remained constant in February, had a small dip in March and increased slowly before the first peak in mid-May. Temperatures then had a steady increase before reaching the highest temperatures in late June.

Turbidity showed the highest peak in early March, indicating rougher weather in this period. The turbidity decreased after this peak, and some smaller peaks were observed in April before a consistent turbidity was observed in the later months of sampling.

Chl *a* concentration (Figure 11) exhibited a pattern with low values in March and April before the spring bloom. Chl *a* values steadily increased in early April, reaching its spring bloom peak 7th of April (7.38 mg.m^{-3}) before plateauing in late April. Followed by a steady decrease towards the beginning of May and keeping a steady concentration from mid-May to mid-June, before a further decrease in late June.

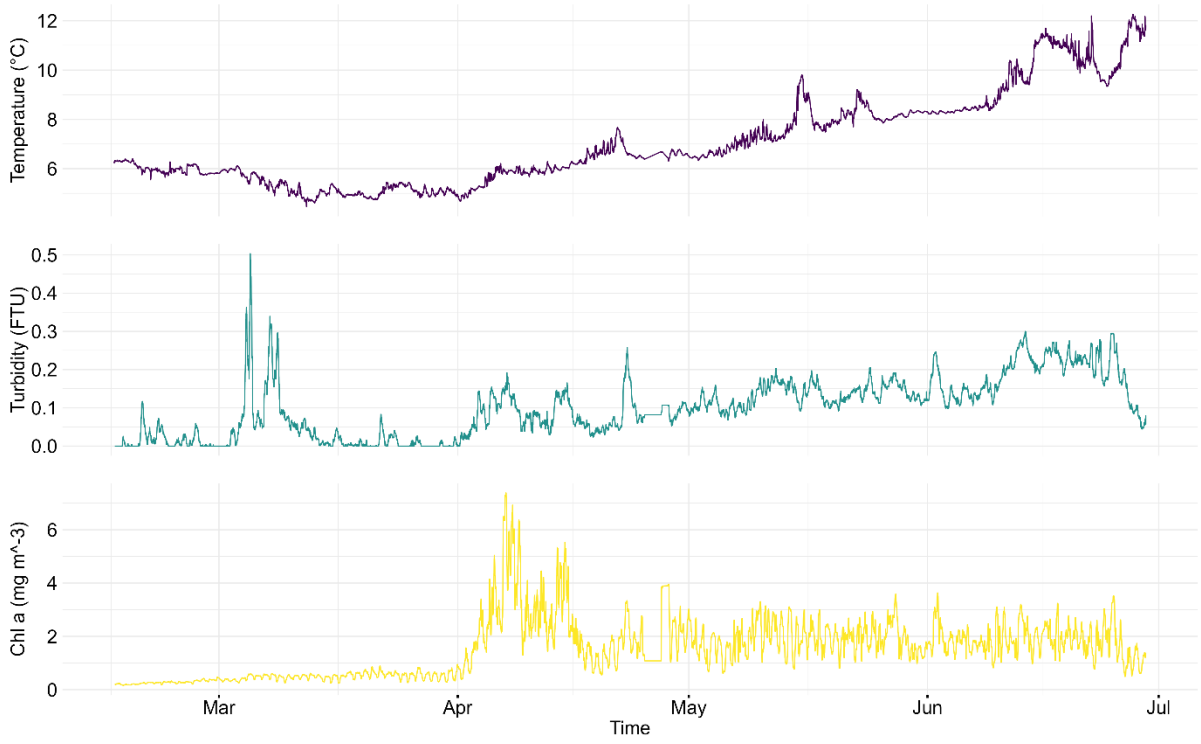

Figure 11: Time series data showing seawater temperature (in Celsius), chlorophyll *a* fluorescence (mg.m^3) and turbidity (Formazin Turbidity Unit) collected every 10-min using the C3 submersible fluorometer at Måsskjæra farm (station MI, inside the farm) from February 16th to June 29th. Note: Different y-axis scales in the two panels.

3.1.3 Nutrients

Concentrations of NH_4 and NO_3 at station MI and MO throughout the sampling period are shown in Figure 12.

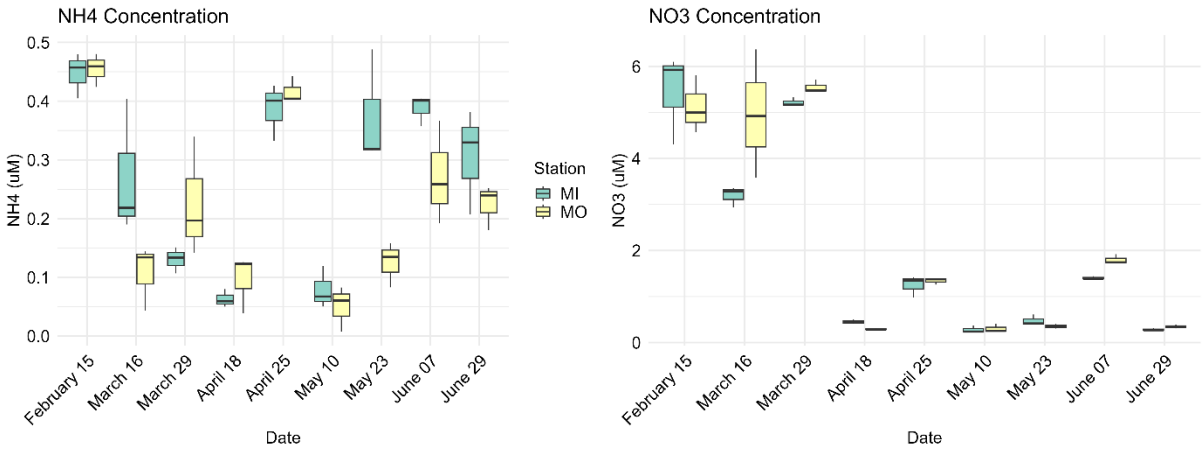

Figure 12: Nutrient concentrations for ammonium, NH_4, and nitrate, NO_3, at sampling dates at station MI (inside the farm) and MO (outside the kelp farm). The boxplot shows the maximum and minimum values (whiskers), the lower and upper quartiles (box), and the median (horizontal line). Note: Different y-axis scales in the two panels.

Nutrient levels of [NH_4] and [NO_3] varied throughout the sampling period as a response to the natural yearly cycles of nutrient concentrations and flows. NO_3 and NH_4 concentrations showed similar trends for station MI and MO. No significant difference in NH_4 (Mann-Whitney U test, p = 0.30) and NO_3 (Mann-Whitney U test, p = 1) concentrations between stations was shown (Figure 12). The concentration of NH_4 was highest on February 15th (mean = 0.45 µM, SD ± 0.03), followed by an instant decrease that lasted until after the spring bloom where it hit another peak. The lowest concentration observed the 10th of May (mean = 0.07 µM, SD ± 0.04) and increased again later in the sampling period.

NO_3 exhibited high concentration values in the beginning of the sampling period. The highest concentration was reached 29th of March (mean = 5.39 µM, SD ± 0.21), followed by a notably decline after the spring bloom (Figure 11). The lowest concentration was also observed 10th of May for NO_3 (mean = 0.29 µM, SD ± 0.08). The concentrations of NO_3 show an inverse correlation with temperature. In end of March, the temperature was between 4°C and 5 °C while the concentrations of NO_3 were at its highest. In June, the temperature showed an increase to around 11°C, while the ambient concentrations of NO_3 were close to depleted (Figure 11)(Figure 12).

3.2 Bryozoan larval abundance

Figure 13 show how the average abundance of cyphonautes of *M. membranacea* and *E. pilosa* change over time at both sampling stations in the sampling period. At station MI, cyphonautes of *E. pilosa* showed a peak in abundance on April 18th with a large standard deviation (mean = 238 ind.m^{-3}, SD ± 173) (Figure 13). Another peak was observed June 29th (mean = 153 ind.m^{-3}, SD ± 71). Cyphonautes of *M. membranacea* showed an increase in abundance over time at station MI, reaching its highest on June 29th (mean = 428 ind.m^{-3}, SD ± 37). A smaller peak was observed on May 10th (mean = 201 ind.m^{-3}, SD ± 68). The lowest abundance was observed 15th of February (mean = 1 ind.m^{-3}, SD ± 0.92 ind.m^{-3}). Cyphonaute larval abundance appeared to be less variable among replicates of *M.*

membranacea compared to *E. pilosa*, especially during peak abundance times. For *M. membranacea* larvae, while there is some variability, the replicates tend to be more consistent.

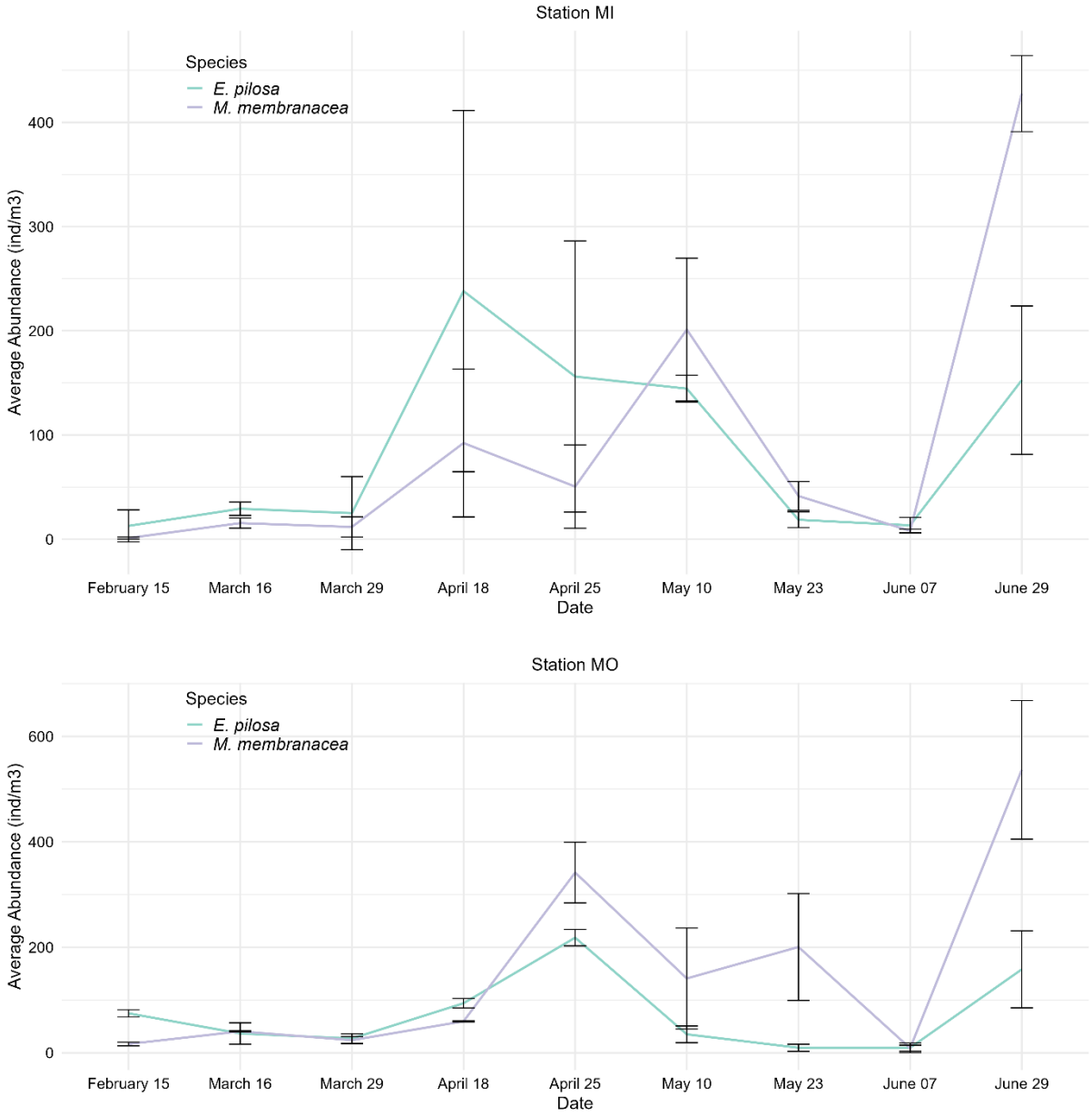

Figure 13: Average abundance (individuals per cubic meter) of *Membranipora membranacea* (purple line) and *Electra pilosa* (green line) at Station MI (inside farm) and MO (outside the kelp farm). Data points represent average abundances calculated from multiple replicates on each sampling date. Error bars indicate the standard deviation. Note: Different y-axis scales are used in the two panels.

At station MO both species had relatively low abundances in the start of the sampling period. *E. pilosa* peaked in abundance in the middle of the sampling period with the highest abundance recorded on April 25th (mean = 218 ind.m^{-3}, SD ± 16). The following sampling days the abundance decreased before it increased again on June 29th (mean = 158 ind.m^{-3}, SD ± 73). *M. membranacea* had a steady increase and peaked in abundance on June 29th (mean = 536 ind.m^{-3}, SD ± 131).

The difference between cyphonaute abundance was not statistically significant between localities for *E. pilosa* (Mann-Whitney U test, p = 0.86), *and M. membranacea* (Mann-Whitney U test, p = 0.11).

Figure 14 shows the change in cyphonaute abundance over time compared to the abundance coverage of encrusted larval colonies that had settled on the seaweed lamina during the same period.

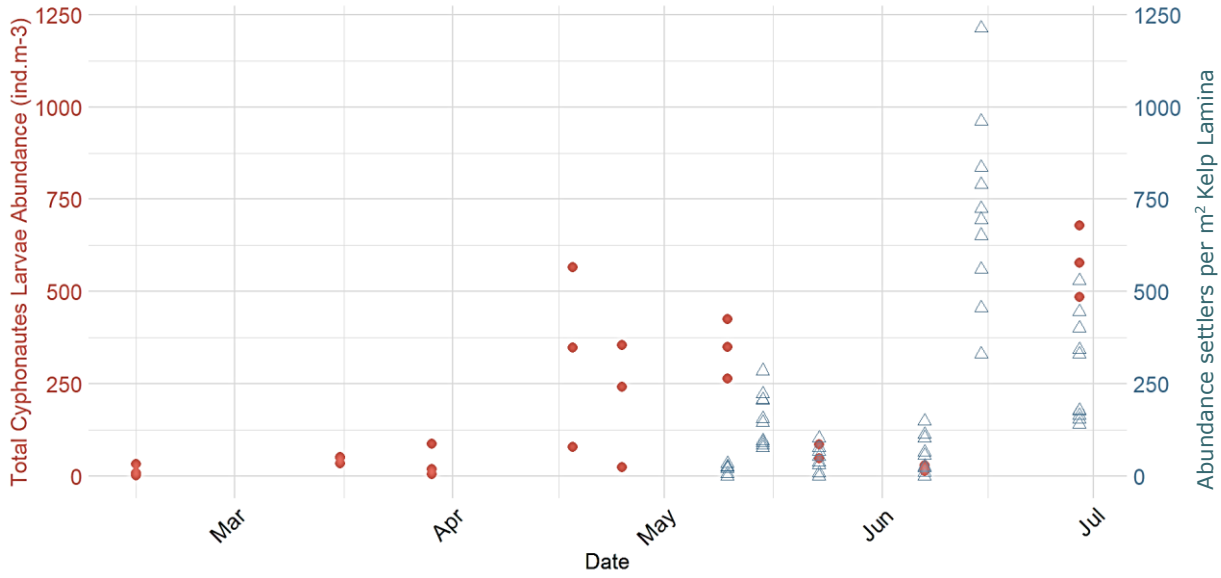

Figure 14: Abundance settlers (m^2) of bryozoan colonies on kelp sampled at station MI (inside the farm), during the same time period as cyphonaute larval abundance in the water. Abundance settlers (blue triangles) show the calculated abundance of settled larvae encrusted per m^2 of sampled kelp. The red dots show the total bryozoan cyphonaute larval abundance in the water column during the same sampling period. More in depth results on bryozoan coverage on kelp was investigated during this project. A detailed description will be found in the master thesis of Elisabeth Alice Snijder, which is under preparation (Snijder, 2024).

The settled larval colonies appeared on the seaweed with a peak in May, and a bigger peak later in June. The abundance of cyphonautes in the water increased towards a peak in late April and the beginning of May, before it decreased in early June. The first settlements of larval colonies on the seaweed were also observed in beginning of May. The abundance of cyphonautes in the water showed a dip during the same time as the first peak of larval colonies encrusted on the kelp. Both the abundance of cyphonautes in the water and recruited larval colonies encrusted on the kelp was peaking in June (Figure 14).

3.3 Bryozoan larval size

Figure 15 show how the morphological traits: maximum basal edge (in mm) and oral-aboral length (in mm) of *E. pilosa* and *M. membranacea* varied over the sampling period. Each plot represents data collected on sampling dates, highlighting the variability and overall trends in size across the study period.

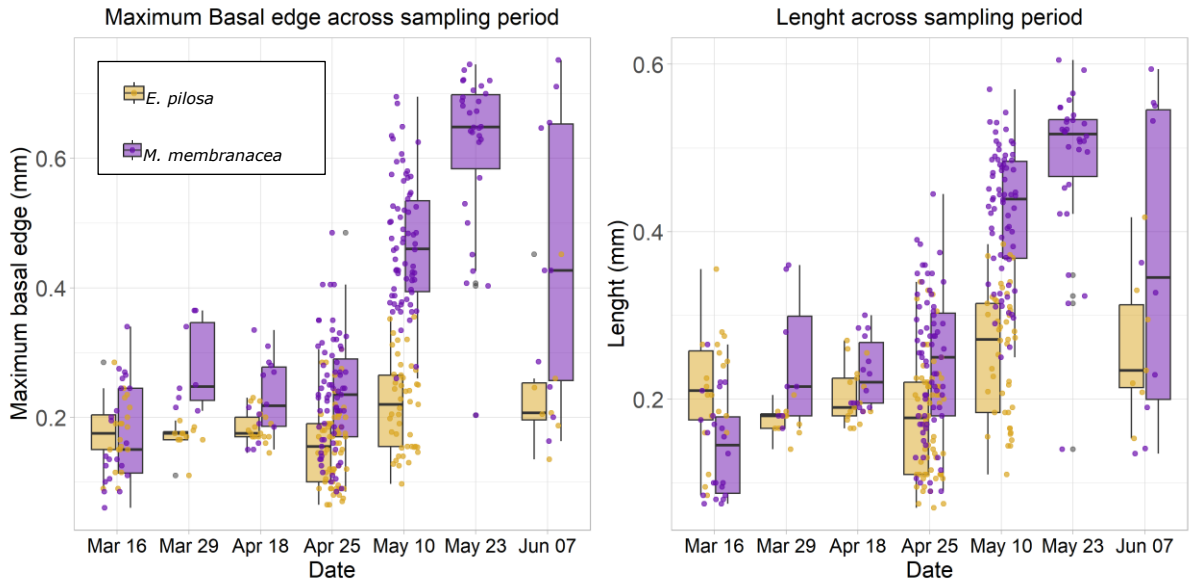

Figure 15: Maximum basal edge (mm) and length of the oral-aboral axis (mm) for *Membranipora membranacea* and *Electra pilosa* sampled with the AFTI-scope. Data for *E. pilosa* on May 23rd is excluded due to lack of data. Box plots show the maximum and minimum values (whiskers), the lower and upper quartiles (box), and the median (horizontal line). Outliers are represented as individual points. Note: Different y-axis scales in the two panels.

Bryozoan larvae of *E. pilosa* and *M. membranacea* from station MI varied in size over time. *M. membranacea* demonstrated a substantial increase in maximum basal edge, especially noticeable in the later sampling dates: May 10th (mean = 0.47 mm, *n* = 70, SD ± 0.096), May 23rd (mean = 0.62 mm, *n* = 30, SD ± 0.13) and June 7th (mean = 0.45, *n* = 10, SD ± 0.22). *M. membranacea* also increased with size in the oral-aboral length. For *E. pilosa* the size growth was more stable (Figure 15).

Some dates showed larger variation in size between the two species. On March 16th the basal edges were quite similar between *E. pilosa* (mean = 0.17 mm, *n* = 20, SD ± 0.05) and *M. membranacea* (mean = 0.18 mm, *n* = 22, SD ± 0.08) but by June 7th, *M. membranacea* showed notably larger maximum basal edge.

In general, the values of *M. membranacea* tended to have larger standard deviations, indicating a broader range of sizes among individuals sampled on those dates, especially on June 7th, when sizes showed a large variation (Figure 15).

3.4 AFTI-scope

The abundance estimates from station MI for *E. pilosa* and *M. membranacea* obtained using AFTI-scope was compared with microscopic counts in Figure 16.

The difference in estimates differed for the two species. The variation in sampling method were most distinct the 18th of April, 25th of April and 10th of May of April for *E.pilosa*. For *M. membranacea* the two methods had the biggest difference in estimates 25th of April and 10th of May (Figure 16).

On average the AFTI-scope estimates were lower than the same samples counted in the microscope. The difference in the abundance estimates for both methods gave a mean difference of -36 ind.m^{-3}. The median difference was -3.98 ind.m^{-3}, suggesting a smaller disparity for many of the samples. The AFTI-scope underestimated the abundance in 66% of the samples (*n* = 21) compared to the microscopic method. The impact of this, however, varied across samples.

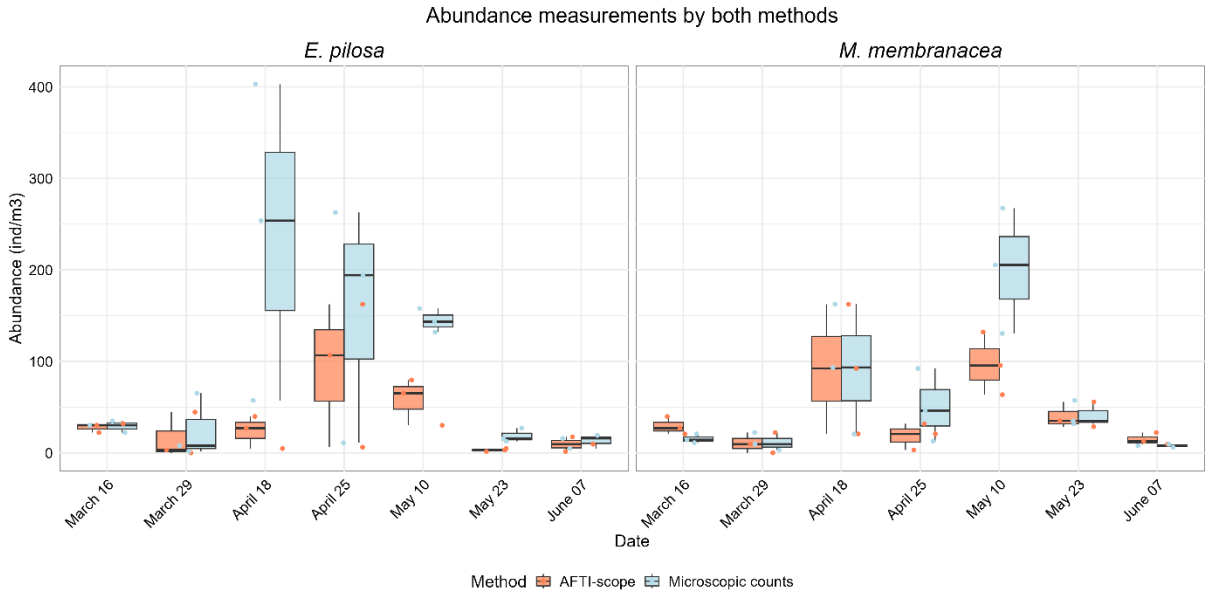

Figure 16: Abundance (ind.m^{-3}) measured for *Electra pilosa* and *Membranipora membranacea* over several sampling dates. AFTI-scope (orange) and microscopic (blue) abundance estimates were compared for accuracy of counting between the two methods. The boxplot shows the maximum and minimum values (whiskers), the lower and upper quartiles (box), and the median (horizontal line). Outliers are represented as individual points.

A significant difference was found in the abundance estimates provided by the AFTI-scope and traditional microscope methods across all samples, irrespective of the species (Wilcoxon signed-rank test, p = 0.00017). Further differentiating was done to look for difference in the methods for each species. For *E. pilosa*, the two methods gave a significant difference in the abundance estimates (Wilcoxon signed-rank test, p = 0.00013). For *M. membranacea* there were no significant difference in the abundance estimates done by the two methods for this species (Wilcoxon signed-rank test, p = 0.287). This was also proved as *E. pilosa* proved to be underestimated in 19 of the 21 samples (90%), however *M. membranacea* was underestimated in 9 of the 91 samples (43%).

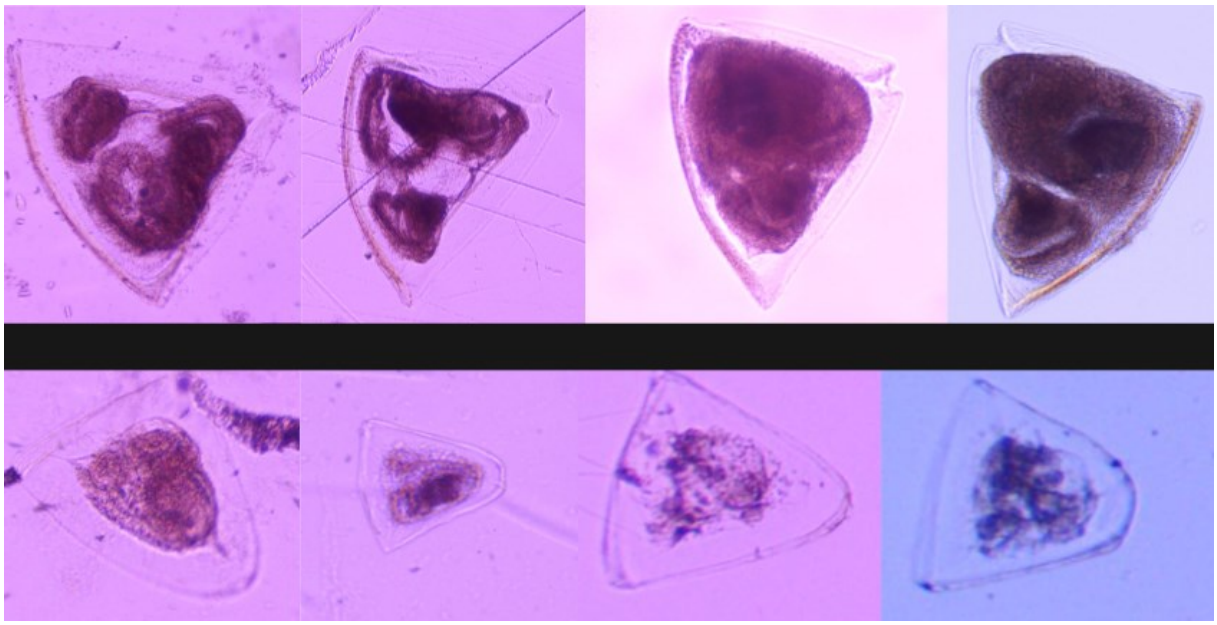

Figure 17: Examples of pictures taken by the AFTI-scope. *Membranipora membranacea* individuals on the upper row and *Electra pilosa* on the bottom row.

3.5 Correlation of environment with bryozoan larval abundance and size

The following figures present heatmaps displaying correlation coefficients between the abundance of *M. membranacea* and *E. pilosa* (individuals per m³) and size measurements with several environmental parameters measured over the study period. The parameters include water temperature (°C), turbidity (FTU), and chlorophyll a concentration (mg.m^{-3}) *in vitro*). Color intensity corresponds to the strength of the correlation, with red indicating positive correlations and blue indicating negative correlations.

Figure 18: Spearman correlation plot of environmental factors and abundance of Electra pilosa (individuals per m³) at station MI and station MO. Colored squares refer to statically significant ($p < 0.05$) positive (red) and negative (blue) correlations for each combination. The value shows the strength of correlation. All environmental factors are averages including three days before the sampling day as the abundance are measured.

Pairwise correlation showed that environmental factors have varying influence on the abundance of bryozoan larvae. A minor negative correlation between *E. pilosa* abundance and both turbidity (-0.07) and chlorophyll a concentration (-0.04) was observed ($p < 0.05$, Spearman correlation, Figure 18). Temperature showed no influence on the abundance of *E. pilosa*.

Turbidity and chlorophyll showed an expected strong positive correlation (Figure 18), displayed as in increase in the concentration of chlorophyll a increased as the water became more turbid.

M. membranacea abundance showed a moderate positive correlation with various environmental variables. The abundance showed a moderate positive correlation with

turbidity (0.38). As well as a mild positive correlation with FChl a (0.22). The relationship with Chl a *in vitro* concentration was similarly moderate (0.37), indicating a potential link between the abundance of *M. membranacea* and primary productivity. (Figure 19).

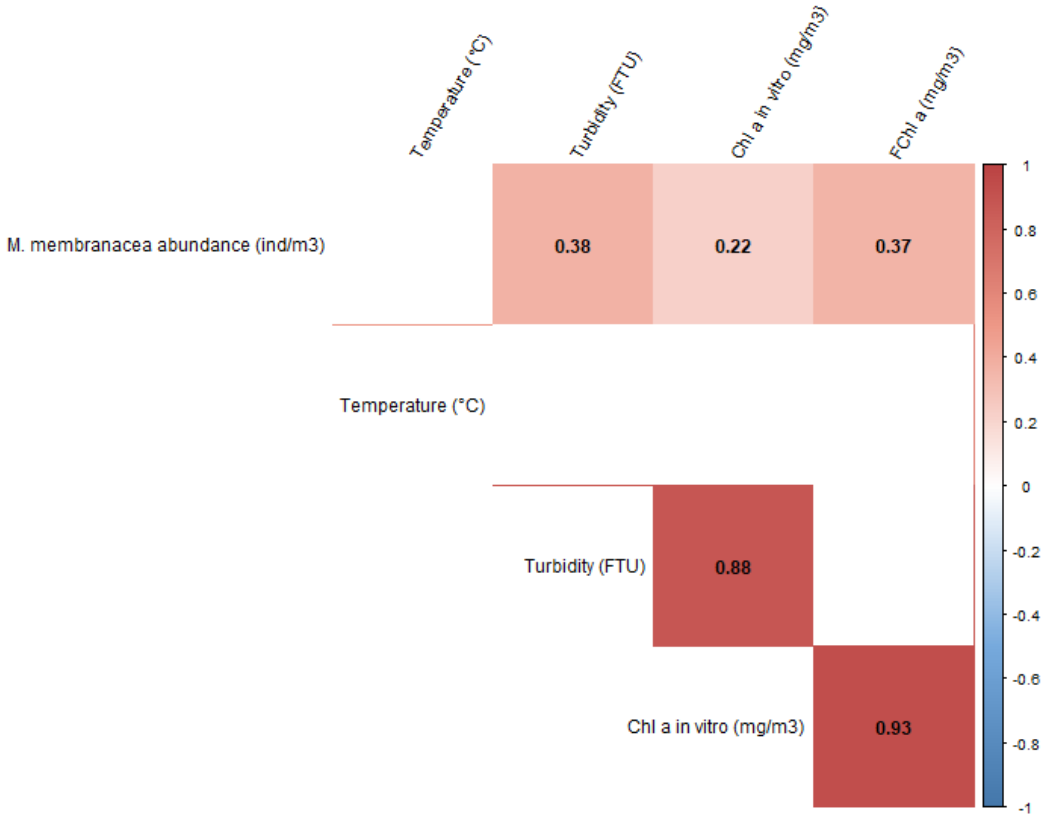

Figure 19: Spearman correlation plot of environmental factors and abundance of *Membranipora membranacea* (individuals per m³) at station MI and station MO. Colored squares refer to statically significant ($p < 0.05$) positive (red) and negative (blue) correlations for each combination. The value shows the strength of correlation.

Moderate correlations were found between *M. membranacea* morphometric measurements and the temperature (0.49 for both). In contrast, the oral-aboral length measurements of *E. pilosa* correlated significantly with the temperature (0.83). (Figure 20).

Overall, a positive correlation between size and temperature was detected, but not necessarily for abundance, as that only showed a moderate positive correlation with *M. membranacea* (Figure 20).

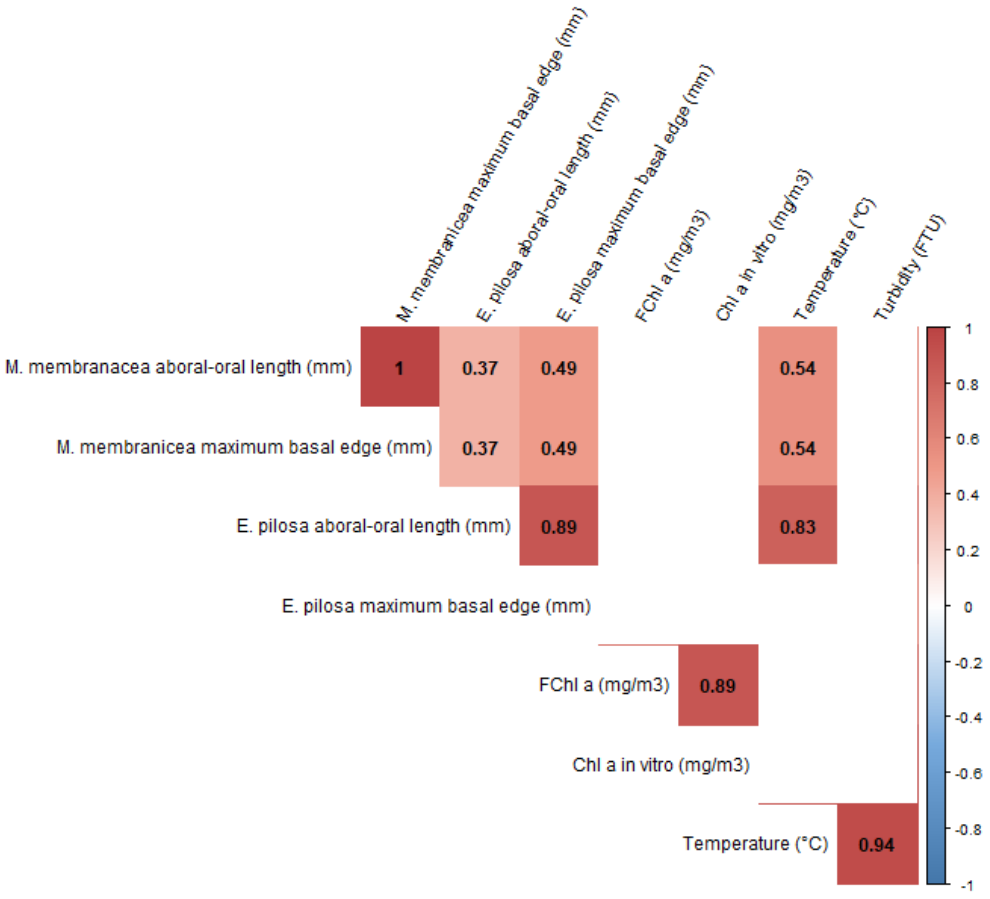

Figure 20: Spearman correlation plot of environmental factors and morphometric measurements (maximum basal edge and oral-aboral length in mm) of Membranipora membranacea and Electra pilosa at station MI. Colored squares refer to statically significant ($p < 0.05$) positive (red) and negative (blue) correlations for each combination. The value shows the strength of correlation.

4 Discussion

4.1 AFTI-scope

Imaging technologies have been popular within the last decade for estimating zooplankton abundances for many zooplankton species, including copepods (Naito et al., 2019), euphausiids (Gorsky et al., 2010) and ichthyoplankton (Williamson et al., 2022). This study explored the use of a flow-through microscope (AFTI-scope) as an optical method for estimation of bryozoan (*E. pilosa* and *M. membranacea*) larvae abundance and size development, for early biofouling detection in a seaweed farm. The AFTI-scope is a novel design built for research purposes and is cost-effective (approximately 1800 €) (Haugum et al., 2023) compared to other commercial imaging systems such as the FlowCytoBot (approximate USD 158 000 $) (Lombard et al., 2019) or the ZooScan (approximate 55 000 €) (Hydroptic, personal communication 03.05.2024). An advantage with the AFTI-scope is the setup of the method. It was easy to handle, as only the instrument and a pc is needed. The user interface provided, made it possible to control the adjustments from the PC, such as the speed of the pump, the number of pictures imaged and the light settings. This made it user-friendly with potential to be used by seaweed farmers. The seaweed farmers could collect images and store information on cyphonaute abundance and growth through the cultivation season over several years and for several locations. This could possibly provide a sufficient dataset on the condition of local bryozoan larvae in a seaweed farm. The ability to collect and store permanent digital information has been pointed out as one of the great advantages with imaging systems like the AFTI-scope (Orenstein et al., 2022).

Another highlight of the study was the high-quality pictures of bryozoan larvae (cyphonautes) throughout the sampling period. Due to the setup of the AFTI-scope the stepper motors gave accurate control of the objects position and focus. The light source was also fixed. This improved the consistency of the experiment by constantly having the same settings. This made it possible to capture high resolution images of the cyphonautes over the sampling period, giving insight into the development of cyphonautes in the early stages and by the time they were mature enough to settle on the kelp. Such a time series is yet to be done in order to get ecological insights into the growth of bryozoan larvae while they are in the planktonic stage. Grandremy et al. (2023) highlighted how copepods imaged with the optical system ZooScan was better at identifying calanoids to the family level compared to other methods. The channel slide made the number of objects captured under the lens limited, and thus made it easier to detect bryozoan larvae with the naked eye when estimating abundance for each sample. This method would not be as suitable with imaging systems like the ZooScan that provide a single image with up to 1500–2000 organisms (Grandremy et al., 2023).

Although this method showed great potential in estimating bryozoan larval abundance, the results revealed a degree of underestimation. On average the AFTI-scope estimates were 26 % lower than the same samples counted in the microscope. Underestimation of zooplankton abundances using other imaging systems was also consistent in other studies. For example, Naito et al. (2019) observed underestimation of zooplankton abundances with an optical scanning image analysis system called Optical Plankton Recorder (OPC). In the same study by Naito et al. (2019) the ZooScan, another optical scanning image analysis

system, was shown to underestimate the abundance of jellyfishes, chaetognaths, polychaete, and barnacle larvae, but significant linear correlations (p = 0.0001) with microscopic observations for the abundance of appendicularians, euphausiids, and copepods were observed. The result from this study showed different estimates from the AFTI-scope between the two species. For *E. pilosa*, the AFTI-scope and traditional counts yielded significantly different abundance estimates, while for *M. membranacea*, the estimates were not significantly different, indicating that the AFTI-scope might need fine-tuning in order to observe *E. pilosa* in the same degree as *M. membranacea*. Bryozoan larvae of *M. membranacea* might have been easier to detect due to their bigger size. *E. pilosa* cyphonautes were smaller and appeared to be more transparent (Figure 17). Despite this, it is known that manual counting under a microscope is labor-intensive and can lead to overestimated abundances due to several factors related to sample preparation, handling, and counting techniques (Longhurst & Seibert, 1967). Based on this there might be potential to continue to develop the AFTI-scope towards a species-specific instrument, fine-tuned for bryozoan larvae, as optical systems have proven to yield different results based on the species sampled (Grandremy et al., 2023; Pitois et al., 2018).

As this study represents the first evaluation of the AFTI-scope for estimating bryozoan larvae, several modifications can enhance the instrument's suitability for application in seaweed farming. The main issue with the use of AFTI-scope was the clogging of the tubes from the inlet syringe to the microscope channel slide due to the amount of biological material that got pumped into the flow cell. The AFTI-scope ensured consistent focal imaging of bryozoan larvae and similar to other closed system it is constrained by the inlet diameter (Colas et al., 2018). The inlet size of the AFTI-scope primarily determined the maximum size of imaged particles, and thus the corresponding volume of biological matter. The amount of detritus and biological material has proven to be a problem when conducting accurate zooplankton abundance estimates in similar imaging plankton technologies (Zhang et al., 2000). In fact, Naito et al. (2019) confirmed that detrital materials were composed 88.2% (SD ± 12.7) of total particles in images sampled with the plankton imager ZooScan. Zhang et al. (2000) concluded that the OPC was only able to produce accurate estimates of zooplankton abundance in water with background detritus <100 particles L^{-1} because high abundance of detrital particles interfered with zooplankton detection, leading to significant measurement errors due to particle coincidence and background noise. In this study the difference in abundance estimates between the AFTI-scope and microscopic counts were most present in the samples densely populated with biological matter, coincidently with the post-peak in phytoplankton bloom. Previous studies done by (Sprules et al., 1998), suggested that the presence of detrital particles to be the largest source of bias for OPC estimates of zooplankton abundance. The findings of this study strengthen and expand upon the existing knowledge of the limitations of optical plankton samplers in environments with substantial detrital loads, as previously outlined by (Zhang et al., 2000). Therefore, the results presented here using the AFTI and other imaging systems suggests that care needs to be taken when monitoring zooplankton abundances in productive regions. Seaweed farms are usually situated in coastal, productive waters (Broch et al., 2019), typically characterized by elevated levels of detritus, which could significantly impact the accuracy of biotic assessments conducted using automated zooplankton imaging.

A way to avoid clogging of the system with biological matter was using a mesh to rinse the sample or diluting the sample to get a fitted concentration of particles, as suggested by Zhang et al. (2000). However, this was time-consuming and could potentially lead to loss of individuals. Because this procedure was time-consuming, it was not possible to do more than the seven samples from one of the stations (MI). Another solution for the AFTI-scope might be to adjust the flow through system with a continues flow cell, more similar to the imaging-in-flow system, named FlowCam (Christian et al., 1998). Increasing the size of the inlet size and tubes would potentially make it possible to achieve a semi-automated way to handle the samples without needing to rinse the system for clogged material.

Another challenge was to annotate the size of the bryozoan larvae by hand in ImageJ, which was also a time-consuming task. Semi-automated procedures for zooplankton identification tested on 89,419 images collected in Chesapeake Bay were consistent with visual counts with >80% accuracy for all groups of zooplankton tested (Bi et al., 2015). An automation of cyphonaute detection and size estimates would greatly improve the time of data collection and allow for more samples to be collected. This would give a sufficient overview of the bryozoan abundance and growth within a farm or from multiple farms from several locations. Manual annotation of image data has remained a major bottleneck that requires expert knowledge and lots of time (Kyathanahally et al., 2021). Machine learning has proven to fulfill this need and surpassed previous state-of-the-art classification performance (Orenstein et al., 2022; Zimmerman et al., 2020). As of now the AFTI-scope does not provide automatic taxonomic information, and the images therefore must be manually sorted. By potentially creating a semi-automated sampler that provides a data set with high quality pictures it would be possible to feed into algorithms for sorting out the bryozoan larvae and account for the abundance. Naito et al. (2019) concluded that the ZooScan provided the most accurate abundance due to the advantage of filtering out abiotic particles. A noteworthy remark is that expert zooplankton taxonomists are becoming increasingly rare and expensive (Grandremy et al., 2023). Benchmarking with imaging instruments, and lab-based imaging instruments like done in this study may help seaweed farmers make environmental monitoring more profitable and reduce the economic costs of traditional lab analysis. The study highlighted another valuable aspect of benchmarking imaging instruments and methods. Optical instruments can provide a more comprehensive understanding of reality. This is demonstrated by the size estimates of bryozoan larvae during their growth period in the water column.

4.2 Larval size and settlement on the kelp

In this study, the size of bryozoan larvae was measured by manual annotation in ImageJ with images from the AFTI-scope. Both species exhibited variability in their average sizes (maximum basal edge and oral-aboral length) over the sampling period, suggesting growth and possibly different stages of development (Atkins, 1955). The size of the bryozoans differed much more later in the season. According to Atkins (1955) fully developed *E. pilosa* larvae have been measured at 0.39 mm across the base and 0.36 mm in height. In this study however, the size of *E. pilosa* proved to be smaller (basal edge 0.24 mm SD± 0.10, height 0.27 mm SD ± 0.09). *M. membranacea* have been found to have a basal edge of around 0.75 - 0.8 mm when ready to metamorphose according to (Ryland & Stebbing, 1971). In this study the mean maximum basal edge of *M. membranacea* was 0.62 mm (SD ± 0.13). The range of size found in this study was below the measurements of existing literature. A reason for this might be the lack of a comprehensive study on cyphonautes, where variability in size is reported among seasons and regions.

Snijder (2024) found the first signs of settled bryozoan larvae (pre-ancestrula) on *S. latissima* in late April, followed by two peaks, one in May and one in June (Figure 14). The cyphonautes of both species from the water samples reached their biggest size in late May and beginning of June, supporting existing literature of increasing size of bryozoan cyphonautes and possibly later stage of maturation before metamorphosis occurs (Atkins, 1955; Ryland & Stebbing, 1971).

Bryozoan larvae, similarly to other meroplankton larvae, are able to rapidly respond to environmental cues, such as substrate availability (Strathmann et al., 2008), or chemical signals (Seed & O'Connor, 1981) prior to settlement and metamorphic morphogenesis (Zeng et al., 2022). The fact that the cyphonautes were in high abundance in the water but not settling on the seaweed earlier in the season (early April) suggests that, either the larvae had not reached competence, or some sort of cue necessary for the settlement was lacking (Strathmann et al., 2008). Saunders et al. (2010) observed that settlement of bryozoan larvae occurred as a response to thermal history of the water column, meaning many cumulative days of increased seawater temperature. In the same study by Saunders et al. (2010) there was a positive correlation with increased colony size when a rise in temperature was reported. The pairwise correlations done in this study showed a positive correlation with increased cyphonautes size with temperature, suggesting that warm waters (> 6°C) were an inducing factor for maturity of the larvae. The results showed no correlation between size and chlorophyll a concentration, however. This may suggest a lag between food availability and larval size or that phytoplankton concentrations were sufficient for larval growth. It has been shown that starvation in *M. membranacea* larvae negatively impacted their metamorphic competence (Strathmann et al., 2008) by reducing the size of internal structures, such as the internal sac, and the pyriform organ required for settlement and metamorphosis. Starved cyphonautes that were re-fed have shown to grow back these structures. This, however, often resulted in smaller ancestrula compared to those formed from well-fed larvae with larger internal sacs. In the same study by Strathmann et al. (2008), the size of the larval shell or the lengths of the ciliary bands used in swimming and feeding, however, have not been shown to change in response to food availability. This suggests that the larvae maintain their swimming capacity, important to search for food and that they likely survive in the water for some period. This was supported by the results in this study due to the first cyphonautes being observed in the

water in February, two months prior to settling. This suggest that the size and condition of the larvae at the time of settlement can significantly impact the early growth and viability of the bryozoan colony.

The spring bloom peaked in April (chlorophyll a concentration of 2.3 mg.m^{-3} from the sensor) and remained high in May and June (mean concentration of Chl a 1.9 mg.m^{-3} and 1.8 mg.m^{-3}) respectively. Not much is known about the impact of food quantity and growth of the cyphonautes larvae. However, there has been several studies on the effect of food concentration when the larvae are settled as bryozoan colonies. Riisgård and Goldson (1997) found that 100 % of the zooids in *E. pilosa* were feeding when the phytoplankton concentration was between 0.5 to 5 Chl a µg.L^{-1}. Maximum growth of *E. pilosa* has been measured when Rhodomonas sp. concentrations were between 1000 and 1500 cells.mL^{-1}, which is equivalent to 1.3-1.9 µg.L^{-1} Chl a (Herman, 1988). Hageman et al. (2009) found the lower limit of growth to be near or below 500 cells.ml^{-1} Rhodomonas, equivalent to 0.63 µg.L^{-1} Chl a in controlled conditions. This has also found to be near the lower limit of nutrition concentrations observed in the natural environment of *E. pilosa* (Hageman et al., 2009). Due to the high biological productivity and high values of Chl a concentration in the study area (Fragoso et al., 2019), Chl a, in addition to temperature, might be an inducing factor for the continuous development and maturation of bryozoan larvae. With the sufficient amount of food available, the planktotrophic bryozoan larvae would, therefore, not starve but continue develop as the water gets warmer to successfully go through metamorphose and settle.

The variability in size among cyphonautes was biggest for the individuals sampled in June. By that time there had already been settlement of bryozoan larvae which would have had chance to reproduced free living larvae. It has been proven that the cyphonautes of *M. membranacea* become competent to settle within approximately four weeks (Saunders et al., 2010). There is therefore a possibility that the variation in size increase by time as there might be several new populations of bryozoan larvae of small size in the water column at the same time.

4.3 The relationship between temperature and Chlorophyll a concentration and bryozoan larval abundance

Bryozoan larval abundance had a dip in late May and beginning of June (Figure 13). This was observed at the same time as the first settlement of larvae encrusted on the kelp (Figure 14). This suggested that the decrease of cyphonautes might be due to an increasing number of larvae settling on the kelp in this period, leading to a shift from planktotrophic larvae to encrusted bryozoan on the kelp. The second peak in cyphonaute larvae from the water samples in late June could suggested a burst in new larval production from the colonies that had already settled and matured on the cultivated kelp. Snijder (2024) revealed a rapid increase in percentage coverage on kelp in late June from the same station where samples were collected for larval counts, which might be a result of settled larvae in early June. Another reason for the decrease in bryozoan larvae in June could be due to top-down control by grazing copepods. A previous study done in a nearby region by (Fragoso et al., 2019) showed higher concentrations of copepods, fecal pellets and ammonium during the same time of the year (May/June), indicating that copepods responds fast to food and actively grazes in this region. The results of the images from the AFTI-scope also revealed a large amount of fecal pellets in the samples, particularly in May and June. Ammonium concentrations also increased at the time of the decrease in larvae abundance. This supports the suggestion of high grazing pressure in this region.

Another possible explanation to the sudden increase in cyphonautes might be due to water mixing and larval dilution. In this study, the average windspeed was particularly high (> 10m/s for 6 days) between 24th and 30th of May 2023 (Norwegian Centre for Climate Services, 2023). This peak in wind activity occurred right before the second peak of cyphonautes in June (Figure 14). Physical processes, such as density gradients have been suggested to affect the distribution and abundance of *M. membranacea* and the native *E. pilosa* larvae in St. Margarets Bay, Nova Scotia (Saunders et al., 2010). These authors showed that highest abundances of cyphonautes were shown in the shallower, warmer, and fresher layers when there was a strong pycnocline formed. A pycnocline was formed during the late sampling days in June and indicated that stratification could be a contributing factor for the high cyphonaute abundance sampled.

A study by Yoshioka (1982) on *M. membranacea* settlement on the giant bladder kelp (*Macrocystis pyrifera*) in California showed that temperature and larval abundance played a major role in population fluctuations of *M. membranacea*. Caines and Gagnon (2012) showed the same results with *M. membranacea* on the kelp *S. longicruris* in northern Canada. In this study, however, no correlation between increased temperatures and larval abundance of both species in the water column was found with the spearman correlation. This lack of correlation might be due to the decrease in abundance in late May and beginning of June. However, this study points to the fact that in the beginning of April cyphonaute abundance reached its first peak, but no fouling was observed. This might be due to temperatures, which were still relatively low (~6°C) before the longest peak of the spring bloom which arrived in April. Furthermore, images from the AFTI-scope of the two bryozoan species showed that they were below the size of maturation in April (Atkins, 1955). The increase in temperature may though not be causative, but indirectly affect factors like phytoplankton concentrations, which affects the larval growth by being a source of food for them (Strathmann et al., 2008). A positive correlation was found between the abundance of *M. membranacea*, and Chl a concentration, while no significant relationship was found for abundance of *E. pilosa* and Chl a. This is consistent with a study by Thomason (2023), which also proved correlation between *M. membranacea* abundance and Chl a in the same area in Norway. The findings in the study emphasize the complexity of larval dynamics in coastal marine ecosystems and the role environmental factors play in bryozoan on larval abundance.

4.4 Future perspectives

This study showed the potential in using AFTI-scope to estimate abundance and size of cyphonautes in a seaweed farm. The method showed the potential in further developing the AFTI-scope as a tool for monitoring bryozoan larvae for surveillance of growth (serving as a proxy for competence) and abundance. This will provide the seaweed farmers with more information about the timing of when the larvae are capable to settle. This is crucial for predicting biofouling on seaweed in the future and could create a dataset of information regarding different farms in Norway and within different regions within a farm. The method does need further fine-tuning and adjustment to avoid the complications of clogging and increase efficiency with a higher degree of automatization. Therefore, benchmarking instruments such as the one presented here may help developers to design future instruments that would address technical as well as methodological biases.

More research is needed to understand the underlying factors that make the cyphonautes settle on the kelp. The documentation of size in this study supports earlier studies stating that the cyphonautes stay in the water for some time before they reach a given size before

settlement (Saunders et al., 2010). Several studies suggests that the settlement itself is largely determined by specific cues (Hadfield et al., 2001). Such cues include chemical factors such as nutrient availability and chemoreception (Soule & Soule, 1977) as well as salinity levels in the water (Forbord et al., 2020). There is a need to do more research on the environmental factors affecting the cyphonaute life stages as this can reveal more about the triggering factors of settlement.

Climate change have been proposed to initiate earlier and more abundant outbreaks of the *M. membranacea* (Saunders & Metaxas, 2008). Saunders et al. (2010) showed that warmer temperatures during winter and spring, led to earlier settlement of bryozoan larvae. According to the study, each increase of one degree Celsius resulted in *M. membranacea* beginning to settle on kelp surfaces up to 18 days earlier than under cooler conditions. This suggests that warmer temperatures accelerate the life cycle of the cyphonaut , causing it to reach the settlement phase sooner (Saunders et al., 2010). This could potentially have great impact of timing of harvest in order to avoid biofouling in the future. However, the settlement of larvae is dependent on other environmental variables such as currents and wind. The type of substrate to settle on have also shown to be of importance as *M. membranacea* have shown to prefer *S. latissima* (Førde et al., 2016). Intensive farming of species including *S. latissima* can potentially lead to a higher outbreaks of bryozoan colonies settlement abundance and colony growth due to more available substrate for the larvae to settle on, which in terms can potentially lead to an earlier harvest.

5 Conclusion

This study used the AFTI-scope, a flow-through particle imaging system as a method for efficient count and image sampling of bryozoan larvae in a seaweed farming facility. The results showed that high quality images of bryozoan cyphonautes larvae were obtained. The AFTI-scope proved to underestimate an average abundance of 26 % lower than the same samples counted in the microscope. The accuracy of the optical method was lower for *E. pilosa* as the two methods yielded statistically different abundance estimates while for *M. membranacea* the method showed no significant difference in the estimates, proving suitable detection capabilities for this species with the current AFTI-scope settings.

The AFTI-scope provided pictures of the bryozoan larvae, revealing growth throughout the sampling period. The cyphonautes of both species reached their biggest size in late May and beginning of June. This was followed by two peaks in abundance for settled bryozoan larvae on *S. latissima*, one in May and one in June. The size of the cyphonautes therefore seemed to correspond to when the bryozoans were mature enough to settle on the kelp. The observed increase in size variation among individual larvae later in the season, could suggest growth and possibly different stages of development. This was potentially linked to environmental conditions such as temperature, which showed a positive correlation with larval size. No correlation was found between bryozoan size and chlorophyll concentrations, suggesting that existing phytoplankton levels could have been sufficient for bryozoan growth.

Bryozoan larvae in the water increased in abundance over time, with peaks in April and June. The first peak was observed after the spring bloom. The second peak in June occurred after the first signs of settlement of larvae on the kelp, suggesting that new populations of larvae had dispersed from the settled colonies. Regarding the relationship between increasing temperature and abundance, no signs of correlation for neither of the species was observed. However, settlement did not occur as larval abundance reached its first peak. This might be due to the cyphonautes not being mature at that point. The results emphasize the use of larval size instead of only abundance on their ability to settle on the kelp lamina.

Consequently, these findings emphasize the complexity of bryozoan larval dynamics in seaweed aquaculture settings and highlight the need for developing specialized instruments on bryozoan larval detection and size estimation in the water column as this could be an important tool related to the timing of settlement on cultivated kelp. AFTI-scope has the potential for further research on the size dependent settlement of bryozoan larvae on cultivated *S. latissima*. Further research on improving the technical limitations can make it less time consuming to provide the data of abundance estimates and size measurement and is thus recommended.

References

Albrecht, M. (2023). A Norwegian seaweed utopia? Governmental narratives of coastal communities, upscaling, and the industrial conquering of ocean spaces. *Maritime Studies*, *22*(3), 37. https://doi.org/10.1007/s40152-023-00324-2

Álvarez, E., Moyano, M., Lopez-Urrutia, A., Nogueira, E., & Scharek, R. (2013). Routine determination of plankton community composition and size structure: A comparison between FlowCAM and light microscopy. *Journal of Plankton Research*. https://doi.org/10.1093/plankt/fbt069

Andersen, G. S., Steen, H., Christie, H., Fredriksen, S., & Moy, F. E. (2011). Seasonal patterns of sporophyte growth, fertility, fouling, and mortality of Saccharina latissima in Skagerrak, Norway: implications for forest recovery. *Journal of Marine Sciences*, *2011*.

Araújo, R., Vázquez Calderón, F., Sánchez López, J., Azevedo, I. C., Bruhn, A., Fluch, S., Garcia Tasende, M., Ghaderiardakani, F., Ilmjärv, T., Laurans, M., Mac Monagail, M., Mangini, S., Peteiro, C., Rebours, C., Stefansson, T., & Ullmann, J. (2021). Current Status of the Algae Production Industry in Europe: An Emerging Sector of the Blue Bioeconomy [Original Research]. *Frontiers in Marine Science*, *7*. https://doi.org/10.3389/fmars.2020.626389

Atkins, D. (1955). The cyphonautes larvae of the Plymouth area and the metamorphosis of Membranipora membranacea (L.). *Journal of the Marine Biological Association of the United Kingdom*, *34*(3), 441-449.

Bannister, J., Sievers, M., Bush, F., & Bloecher, N. (2019). Biofouling in marine aquaculture: a review of recent research and developments. *Biofouling*, *35*(6), 631-648.

Bi, H., Guo, Z., Benfield, M. C., Fan, C., Ford, M., Shahrestani, S., & Sieracki, J. M. (2015). A Semi-Automated Image Analysis Procedure for In Situ Plankton Imaging Systems. *PLOS ONE*, *10*(5), e0127121. https://doi.org/10.1371/journal.pone.0127121

Bojorges, H., Fabra, M. J., López-Rubio, A., & Martínez-Abad, A. (2022). Alginate industrial waste streams as a promising source of value-added compounds valorization. *Science of The Total Environment*, *838*, 156394. https://doi.org/https://doi.org/10.1016/j.scitotenv.2022.156394

Broch, O. J., Alver, M. O., Bekkby, T., Gundersen, H., Forbord, S., Handå, A., Skjermo, J., & Hancke, K. (2019). The kelp cultivation potential in coastal and offshore regions of Norway. *Frontiers in Marine Science*, *5*, 529.

Burki, F., Sandin, M. M., & Jamy, M. (2021). Diversity and ecology of protists revealed by metabarcoding. *Current Biology*, *31*(19), R1267-R1280. https://doi.org/https://doi.org/10.1016/j.cub.2021.07.066

Buschmann, A. H., Camus, C., Infante, J., Neori, A., Israel, Á., Hernández-González, M. C., Pereda, S. V., Gomez-Pinchetti, J. L., Golberg, A., & Tadmor-Shalev, N. (2017). Seaweed production: overview of the global state of exploitation, farming and emerging research activity. *European Journal of Phycology*, *52*(4), 391-406.

Caines, S., & Gagnon, P. (2012). Population dynamics of the invasive bryozoan Membranipora membranacea along a 450-km latitudinal range in the subarctic northwestern Atlantic. *Marine Biology*, *159*, 1817-1832.

Campbell, L. M., Fairbanks, L., Murray, G., Stoll, J. S., D'Anna, L., & Bingham, J. (2021). From Blue Economy to Blue Communities: reorienting aquaculture expansion for community wellbeing. *Marine Policy*, *124*, 104361.

Charrier, B., Abreu, M. H., Araujo, R., Bruhn, A., Coates, J. C., De Clerck, O., Katsaros, C., Robaina, R. R., & Wichard, T. (2017). Furthering knowledge of seaweed growth and development to facilitate sustainable aquaculture. *New Phytologist*, *216*(4), 967-975.

Christian, K. S., Michael, E. S., & Charles, S. Y. (1998). An imaging-in-flow system for automated analysis of marine microplankton. *Marine Ecology Progress Series*, *168*, 285-296. https://www.int-res.com/abstracts/meps/v168/p285-296/

Colas, F., Tardivel, M., Perchoc, J., Lunven, M., Forest, B., Guyader, G., Danielou, M. M., Le Mestre, S., Bourriau, P., Antajan, E., Sourisseau, M., Huret, M., Petitgas, P., & Romagnan, J. B. (2018). The ZooCAM, a new in-flow imaging system for fast onboard counting, sizing and classification of fish eggs and metazooplankton. *Progress in Oceanography*, *166*, 54-65. https://doi.org/https://doi.org/10.1016/j.pocean.2017.10.014

Dixon, J., Schroeter, S. C., & Kastendiek, J. (1981). Effects of the Encrusting Bryozoan, Membranipora membranacea, on the Loss of Blades and Fronds by the Giant Kelp, Macrocystis pyrifera (Laminariales) 1. *Journal of Phycology*, *17*(4), 341-345.

Duarte, C. M., Wu, J., Xiao, X., Bruhn, A., & Krause-Jensen, D. (2017). Can Seaweed Farming Play a Role in Climate Change Mitigation and Adaptation? [Perspective]. *Frontiers in Marine Science*, *4*. https://doi.org/10.3389/fmars.2017.00100

Ervik, H., Finne, T. E., & Jenssen, B. M. (2018). Toxic and essential elements in seafood from Mausund, Norway. *Environmental Science and Pollution Research*, *25*, 7409-7417.

FAO. (2022). *The State of World Fisheries and Aquaculture 2022. Towards Blue Transformation*. FAO. https://doi.org/https://doi.org/10.4060/cc0461en

Fernand, F., Israel, A., Skjermo, J., Wichard, T., Timmermans, K. R., & Golberg, A. (2017). Offshore macroalgae biomass for bioenergy production: Environmental aspects, technological achievements and challenges. *Renewable and Sustainable Energy Reviews*, *75*, 35-45.

Fiskeridirektoratet. (2022a, 10.12.2023). *Algae. Harvesting of farmed algae. Quantity in metric tons. Value in 1000 NOK* Fiskeridirektoratet. Retrieved 08.04.2024 from https://www.fiskeridir.no/Akvakultur/Tall-og-analyse/Akvakulturstatistikk-tidsserier/Alger

Fiskeridirektoratet. (2022b, 25.01.2024). *Algea. Number of licences per 31 December by county*. Fiskeridirektoratet. Retrieved 08.04.2024 from https://www.fiskeridir.no/Akvakultur/Tall-og-analyse/Akvakulturstatistikk-tidsserier/Alger

Fiskeridirektoratet. (2022c, 12.10.2023). *Algea.Number of companies and licenses with production by county*. Fiskeridirektoratet. Retrieved 08.04.2024 from https://www.fiskeridir.no/Akvakultur/Tall-og-analyse/Akvakulturstatistikk-tidsserier/Alger

Forbord, S., Matsson, S., Brodahl, G. E., Bluhm, B. A., Broch, O. J., Handå, A., Metaxas, A., Skjermo, J., Steinhovden, K. B., & Olsen, Y. (2020). Latitudinal, seasonal and depth-dependent variation in growth, chemical composition and biofouling of cultivated Saccharina latissima (Phaeophyceae) along the Norwegian coast. *Journal of applied phycology*, *32*(4), 2215-2232. https://doi.org/10.1007/s10811-020-02038-y

Forbord, S., Skjermo, J., Arff, J., Handå, A., Reitan, K. I., Bjerregaard, R., & Lüning, K. (2012). Development of Saccharina latissima (Phaeophyceae) kelp hatcheries with year-round production of zoospores and juvenile sporophytes on culture ropes for kelp aquaculture. *Journal of applied phycology*, *24*, 393-399.

Fragoso, G. M., Davies, E. J., Ellingsen, I., Chauton, M. S., Fossum, T., Ludvigsen, M., Steinhovden, K. B., Rajan, K., & Johnsen, G. (2019). Physical controls on phytoplankton size structure, photophysiology and suspended particles in a Norwegian biological hotspot. *Progress in Oceanography*, *175*, 284-299. https://doi.org/https://doi.org/10.1016/j.pocean.2019.05.001

Fuchs, J., Martindale, M. Q., & Hejnol, A. (2011). Gene expression in bryozoan larvae suggest a fundamental importance of pre-patterned blastemic cells in the bryozoan life-cycle. *EvoDevo*, *2*(1), 13. https://doi.org/10.1186/2041-9139-2-13

Førde, H., Forbord, S., Handå, A., Fossberg, J., Arff, J., Johnsen, G., & Reitan, K. I. (2016). Development of bryozoan fouling on cultivated kelp (Saccharina latissima) in Norway. *Journal of applied phycology*, *28*, 1225-1234.

Getachew, P., Kang, J.-Y., Choi, J.-S., & Hong, Y.-K. (2015). Does bryozoan colonization alter the biochemical composition of Saccharina japonica affecting food safety and quality? *Botanica Marina*, *58*(4), 267-274.

Gorsky, G., Ohman, M. D., Picheral, M., Gasparini, S., Stemmann, L., Romagnan, J.-B., Cawood, A., Pesant, S., García-Comas, C., & Prejger, F. (2010). Digital zooplankton image analysis using the ZooScan integrated system. *Journal of Plankton Research*, *32*(3), 285-303. https://doi.org/10.1093/plankt/fbp124

Grandremy, N., Dupuy, C., Petitgas, P., Mestre, S. L., Bourriau, P., Nowaczyk, A., Forest, B., & Romagnan, J. B. (2023). The ZooScan and the ZooCAM zooplankton imaging systems are intercomparable: A benchmark on the Bay of Biscay zooplankton. *Limnology and Oceanography: Methods*, *21*(11), 718-733.

Hadfield, M. G. (2000). Why and how marine-invertebrate larvae metamorphose so fast. Seminars in cell & developmental biology,

Hadfield, M. G., Carpizo-Ituarte, E. J., Del Carmen, K., & Nedved, B. T. (2001). Metamorphic competence, a major adaptive convergence in marine invertebrate larvae. *American Zoologist*, *41*(5), 1123-1131.

Hadjimichael, M. (2018). A call for a blue degrowth: unravelling the European Union's fisheries and maritime policies. *Marine Policy*, *94*, 158-164.

Hageman, S. J., Needham, L. L., & Todd, C. D. (2009). Threshold effects of food concentration on the skeletal morphology of the bryozoan Electra pilosa (Linnaeus, 1767). *Lethaia*, *42*(4), 438-451.

Haugum, M. (2022). *Designing a Flow-Through Particle Imaging System for Autonomous Surface Vehicles* NTNU].

Haugum, M., Fragoso, G. M., Henriksen, M. B., Zolich, A. P., & Johansen, T. A. (2023). Autonomous Flow-Through RGB and Hyperspectral Imaging for Unmanned Surface Vehicles. OCEANS 2023-Limerick,

Herman, A. W. (1988). Simultaneous measurement of zooplankton and light attenuance with a new optical plankton counter. *Continental Shelf Research*, *8*(2), 205-221.

Holdt, S. L., & Kraan, S. (2011). Bioactive compounds in seaweed: functional food applications and legislation. *Journal of applied phycology*, *23*(3), 543-597. https://doi.org/10.1007/s10811-010-9632-5

Hurd, C. L., Durante, K. M., & Harrison, P. J. (2000). Influence of bryozoan colonization on the physiology of the kelp Macrocystis integrifolia (Laminariales, Phaeophyta) from nitrogen-rich and-poor sites in Barkley Sound, British Columbia, Canada. *Phycologia*, *39*(5), 435-440.

Hwang, E. K., Yotsukura, N., Pang, S. J., Su, L., & Shan, T. F. (2019). Seaweed breeding programs and progress in eastern Asian countries. *Phycologia*, *58*(5), 484-495. https://doi.org/10.1080/00318884.2019.1639436

Jevne, L. S., Guttu, M., Båtnes, A. S., Olsen, Y., & Reitan, K. I. (2021). Planktonic and Parasitic Sea Lice Abundance on Three Commercial Salmon Farms in Norway Throughout a Production Cycle. *Frontiers in Marine Science*, *8*, 615567.

Jiang, Z., Liu, J., Li, S., Chen, Y., Du, P., Zhu, Y., Liao, Y., Chen, Q., Shou, L., Yan, X., Zeng, J., & Chen, J. (2020). Kelp cultivation effectively improves water quality and regulates phytoplankton community in a turbid, highly eutrophic bay. *Science of The Total Environment*, *707*, 135561. https://doi.org/https://doi.org/10.1016/j.scitotenv.2019.135561

kartverket.no. (2023). *Resultat for Måsskjæra (Hitra)*. https://www.kartverket.no/til-sjos/se-havniva/resultat?id=438628&location=M%C3%A5sskj%C3%A6ra

Keeley, N., Valdemarsen, T., Woodcock, S., Holmer, M., Husa, V., & Bannister, R. (2019). Resilience of dynamic coastal benthic ecosystems in response to large-scale finfish farming. *Aquaculture Environment Interactions*, *11*. https://doi.org/10.3354/aei00301

Kérouel, R., & Aminot, A. (1997). Fluorometric determination of ammonia in sea and estuarine waters by direct segmented flow analysis. *Marine Chemistry*, *57*(3-4), 265-275.

Krause-Jensen, D., & Duarte, C. M. (2016). Substantial role of macroalgae in marine carbon sequestration. *Nature Geoscience*, *9*(10), 737-742. https://doi.org/10.1038/ngeo2790

Krumhansl, K. A., Lee, J. M., & Scheibling, R. E. (2011). Grazing damage and encrustation by an invasive bryozoan reduce the ability of kelps to withstand breakage by waves. *Journal of Experimental Marine Biology and Ecology*, *407*(1), 12-18.

Kraan, S. (2020). Chapter 3 - Seaweed resources, collection, and cultivation with respect to sustainability. In M. D. Torres, S. Kraan, & H. Dominguez (Eds.), *Sustainable Seaweed Technologies* (pp. 89-102). Elsevier. https://doi.org/https://doi.org/10.1016/B978-0-12-817943-7.00003-2

Kyathanahally, S. P., Hardeman, T., Merz, E., Bulas, T., Reyes, M., Isles, P., Pomati, F., & Baity-Jesi, M. (2021). Deep Learning Classification of Lake Zooplankton [Original Research]. *Frontiers in Microbiology*, *12*. https://doi.org/10.3389/fmicb.2021.746297

Lange, L., Bak, U. G., Hansen, S. C. B., Gregersen, O., Harmsen, P., Karlsson, E. N., Meyer, A., Mikkelsen, M. D., Van Den Broek, L., & Hreggviðsson, G. Ó. (2020). Chapter 1 - Opportunities for seaweed biorefinery. In M. D. Torres, S. Kraan, & H. Dominguez (Eds.), *Sustainable Seaweed Technologies* (pp. 3-31). Elsevier. https://doi.org/https://doi.org/10.1016/B978-0-12-817943-7.00001-9

Lombard, F., Boss, E., Waite, A. M., Vogt, M., Uitz, J., Stemmann, L., Sosik, H. M., Schulz, J., Romagnan, J.-B., Picheral, M., Pearlman, J., Ohman, M. D., Niehoff, B., Möller, K. O., Miloslavich, P., Lara-Lpez, A., Kudela, R., Lopes, R. M., Kiko, R., . . . Appeltans, W. (2019). Globally Consistent Quantitative Observations of Planktonic Ecosystems [Review]. *Frontiers in Marine Science*, *6*. https://doi.org/10.3389/fmars.2019.00196

Longhurst, A. R., & Seibert, D. L. (1967). Skill in the use of Folsom's plankton sample splitter 1. *Limnology and Oceanography*, *12*(2), 334-335.

Lüning, K., & Mortensen, L. (2015). European aquaculture of sugar kelp (Saccharina latissima) for food industries: iodine content and epiphytic animals as major problems. *Botanica Marina*, *58*(6), 449-455.

Michelsen, F. A., Klebert, P., Broch, O. J., & Alver, M. O. (2019). Impacts of fish farm structures with biomass on water currents: A case study from Frøya. *Journal of Sea Research*, *154*, 101806.

Naito, A., Abe, Y., Matsuno, K., Nishizawa, B., Kanna, N., Sugiyama, S., & Yamaguchi, A. (2019). Surface zooplankton size and taxonomic composition in Bowdoin Fjord, north-western Greenland: A comparison of ZooScan, OPC and microscopic analyses. *Polar Science*, *19*, 120-129. https://doi.org/https://doi.org/10.1016/j.polar.2019.01.001

Norwegian Centre for Climate Services. (2023). *Observasjoner og værstatistikk [Observations and weather statistics]* Norwegian Centre for Climate Services (NCCS). https://doi.org/https://seklima.met.no/kss

Olafsen, T., Winther, U., Olsen, Y., & Skjermo, J. (2012). Value created from productive oceans in 2050. *SINTEF Fisheries and Aquaculture*, *83*.

Orenstein, E. C., Ayata, S. D., Maps, F., Becker, É. C., Benedetti, F., Biard, T., de Garidel-Thoron, T., Ellen, J. S., Ferrario, F., & Giering, S. L. (2022). Machine learning techniques to characterize functional traits of plankton from image data. *Limnology and Oceanography*, *67*(8), 1647-1669.

Overrein, M. M., Tinn, P., Aldridge, D., Johnsen, G., & Fragoso, G. M. (2024). Biomass estimations of cultivated kelp using underwater RGB images from a mini-ROV and computer vision approaches [Original Research]. *Frontiers in Marine Science*, *11*. https://doi.org/10.3389/fmars.2024.1324075

Padam, B. S., & Chye, F. Y. (2020). Chapter 2 - Seaweed components, properties, and applications. In M. D. Torres, S. Kraan, & H. Dominguez (Eds.), *Sustainable Seaweed Technologies* (pp. 33-87). Elsevier. https://doi.org/https://doi.org/10.1016/B978-0-12-817943-7.00002-0

Pauly, D. (2018). A vision for marine fisheries in a global blue economy. *Marine Policy*, *87*, 371-374.

Peters, L., Spatharis, S., Dario, M. A., Dwyer, T., Roca, I. J. T., Kintner, A., Kanstad-Hanssen, Ø., Llewellyn, M. S., & Praebel, K. (2018). Environmental DNA: A New Low-Cost Monitoring Tool for Pathogens in Salmonid Aquaculture [Original Research]. *Frontiers in Microbiology*, *9*. https://doi.org/10.3389/fmicb.2018.03009

Pitois, S. G., Tilbury, J., Bouch, P., Close, H., Barnett, S., & Culverhouse, P. F. (2018). Comparison of a Cost-Effective Integrated Plankton Sampling and Imaging Instrument with Traditional Systems for Mesozooplankton Sampling in the Celtic Sea [Original Research]. *Frontiers in Marine Science*, *5*. https://doi.org/10.3389/fmars.2018.00005

Pollina, T., Larson, A. G., Lombard, F., Li, H., Le Guen, D., Colin, S., de Vargas, C., & Prakash, M. (2022). PlanktoScope: Affordable Modular Quantitative Imaging Platform for Citizen Oceanography [Methods]. *Frontiers in Marine Science*, *9*. https://doi.org/10.3389/fmars.2022.949428

Pratt, M. C., & Grason, E. W. (2007). Invasive species as a new food source: does a nudibranch predator prefer eating an invasive bryozoan? *Biological Invasions*, *9*, 645-655.

Riisgård, H. U., & Goldson, A. (1997). Minimal scaling of the lophophore filter-pump in ectoprocts (Bryozoa) excludes physiological regulation of filtration rate to nutritional needs. Test of hypothesis. *Marine Ecology Progress Series*, *156*, 109-120.

Ryland, J. (1965). *Polyzoa (Bryozoa). Order Cheilostomata Cyphonautes Larvae*. Conseil International pour l'Exploration de la Mer ICES.

Ryland, J., & Stebbing, A. (1971). Settlement and orientated growth in epiphytic and epizoic bryozoans. Fourth European marine biology symposium. Cambridge University Press, Cambridge,

Saunders, M., & Metaxas, A. (2008). High recruitment of the introduced bryozoan Membranipora membranacea is associated with kelp bed defoliation in Nova Scotia, Canada. *Marine Ecology-progress Series - MAR ECOL-PROGR SER*, *369*, 139-151. https://doi.org/10.3354/meps07669

Saunders, M., Metaxas, A., & Filgueira, R. (2010). Implications of warming temperatures for population outbreaks of a nonindigenous species (Membranipora membranacea, Bryozoa) in rocky subtidal ecosystems. *Limnology and Oceanography*, *55*, 1627-1642. https://doi.org/10.4319/lo.2010.55.4.1627

Seed, R., & O'Connor, R. J. (1981). Community organization in marine algal epifaunas. *Annual Review of Ecology and Systematics*, *12*(1), 49-74.

Skagseth, Ø., Drinkwater, K. F., & Terrile, E. (2011). Wind-and buoyancy-induced transport of the Norwegian Coastal Current in the Barents Sea. *Journal of Geophysical Research: Oceans*, *116*(C8).

Skjermo, J., Aasen, I. M., Arff, J., Broch, O. J., Carvajal, A. K., Christie, H. C., Forbord, , S., O., Y., Reitan, K. I., Rustad, T., Sandquist, J., Solbakken, R., Steinhovden, , & K. B., W., B., Wolff, R., & Handå, A. (2014). *A new Norwegian bioeconomy based on cultivation and processing of seaweeds: Opportunities and R&D needs* (SINTEF A25981).

Snijder, E. A. (2024). *Investigating abiotic and biotic factors related to the growth of bryozoans on kelp lamina (Unpublished master's thesis).* Norwegian University of Science and Technology.

Soule, J. D., & Soule, D. F. (1977). Fouling and bioadhesion: life strategies of bryozoans. *Biology of bryozoans*, 437-457.

Sprules, W., Jin, E., Herman, A., & Stockwell, J. (1998). Calibration of an optical plankton counter for use in fresh water. *Limnology and Oceanography*, *43*(4), 726-733.

Stévant, P., & Rebours, C. (2021). Landing facilities for processing of cultivated seaweed biomass: a Norwegian perspective with strategic considerations for the European seaweed industry. *Journal of applied phycology*, *33*(5), 3199-3214. https://doi.org/10.1007/s10811-021-02525-w

Stévant, P., Rebours, C., & Chapman, A. (2017). Seaweed aquaculture in Norway: recent industrial developments and future perspectives. *Aquaculture International*, *25*(4), 1373-1390. https://doi.org/10.1007/s10499-017-0120-7

Strathmann, R. R., Foley Jr, G. P., & Hysert, A. N. (2008). Loss and gain of the juvenile rudiment and metamorphic competence during starvation and feeding of bryozoan larvae. *Evolution & development*, *10*(6), 731-736.

Sætre, R. (2007). *The Norwegian coastal current: oceanography and climate*. Fagbokforlaget.

Thomason, P. B. (2023). *Bryozoan larvae (cyphonauts) growth and encrustation in Saccharina latissima: analysis of biotic and abiotic interactions* NTNU].

van den Burg, S. W. K., van Duijn, A. P., Bartelings, H., van Krimpen, M. M., & Poelman, M. (2016). The economic feasibility of seaweed production in the North Sea. *Aquaculture Economics & Management*, *20*(3), 235-252. https://doi.org/10.1080/13657305.2016.1177859

Voyer, M., Quirk, G., McIlgorm, A., & Azmi, K. (2018). Shades of blue: what do competing interpretations of the Blue Economy mean for oceans governance? *Journal of environmental policy & planning*, *20*(5), 595-616.

Williamson, D. R., Nordtug, T., Leirvik, F., Kvæstad, B., Hansen, B. H., Ludvigsen, M., & Davies, E. J. (2022). A flow-through imaging system for automated measurement of ichthyoplankton. *MethodsX*, *9*, 101773. https://doi.org/https://doi.org/10.1016/j.mex.2022.101773

Winston, J. E., Woollacott, R., & Zimmer, R. (1977). Feeding in marine bryozoans. *Biology of bryozoans*, *233*, 271.

World Bank. (2023). *Global Seaweed: New and Emerging Markets Report, 2023*. https://openknowledge.worldbank.org/handle/10986/40187

Yoshioka, P. M. (1982). Predator-induced polymorphism in the bryozoan Membranipora membranacea (L.). *Journal of Experimental Marine Biology and Ecology*, *61*(3), 233-242.

Young, N., Sharpe, R. A., Barciela, R., Nichols, G., Davidson, K., Berdalet, E., & Fleming, L. E. (2020). Marine harmful algal blooms and human health: A systematic scoping review. *Harmful Algae*, *98*, 101901. https://doi.org/https://doi.org/10.1016/j.hal.2020.101901

Zeng, Z., Jiang, C., Tan, Q., Tang, B., & Huang, Z. (2022). Larvae of a marine gastropod and a marine bivalve share common gene expression signatures during metamorphic competence. *Marine Biology*, *169*(9), 117. https://doi.org/10.1007/s00227-022-04106-y

Zhang, L., Liao, W., Huang, Y., Wen, Y., Chu, Y., & Zhao, C. (2022). Global seaweed farming and processing in the past 20 years. *Food Production, Processing and Nutrition*, *4*(1), 23. https://doi.org/10.1186/s43014-022-00103-2

Zhang, X., Roman, M., Sanford, A., Adolf, H., Lascara, C., & Burgett, R. (2000). Can an optical plankton counter produce reasonable estimates of zooplankton abundance and biovolume in water with high detritus? *Journal of Plankton Research*, *22*(1), 137-150. https://doi.org/10.1093/plankt/22.1.137

Zimmerman, T. G., Pastore, V. P., Biswas, S. K., & Bianco, S. (2020). Embedded system to detect, track and classify plankton using a lensless video microscope. *arXiv preprint arXiv:2005.13064*.

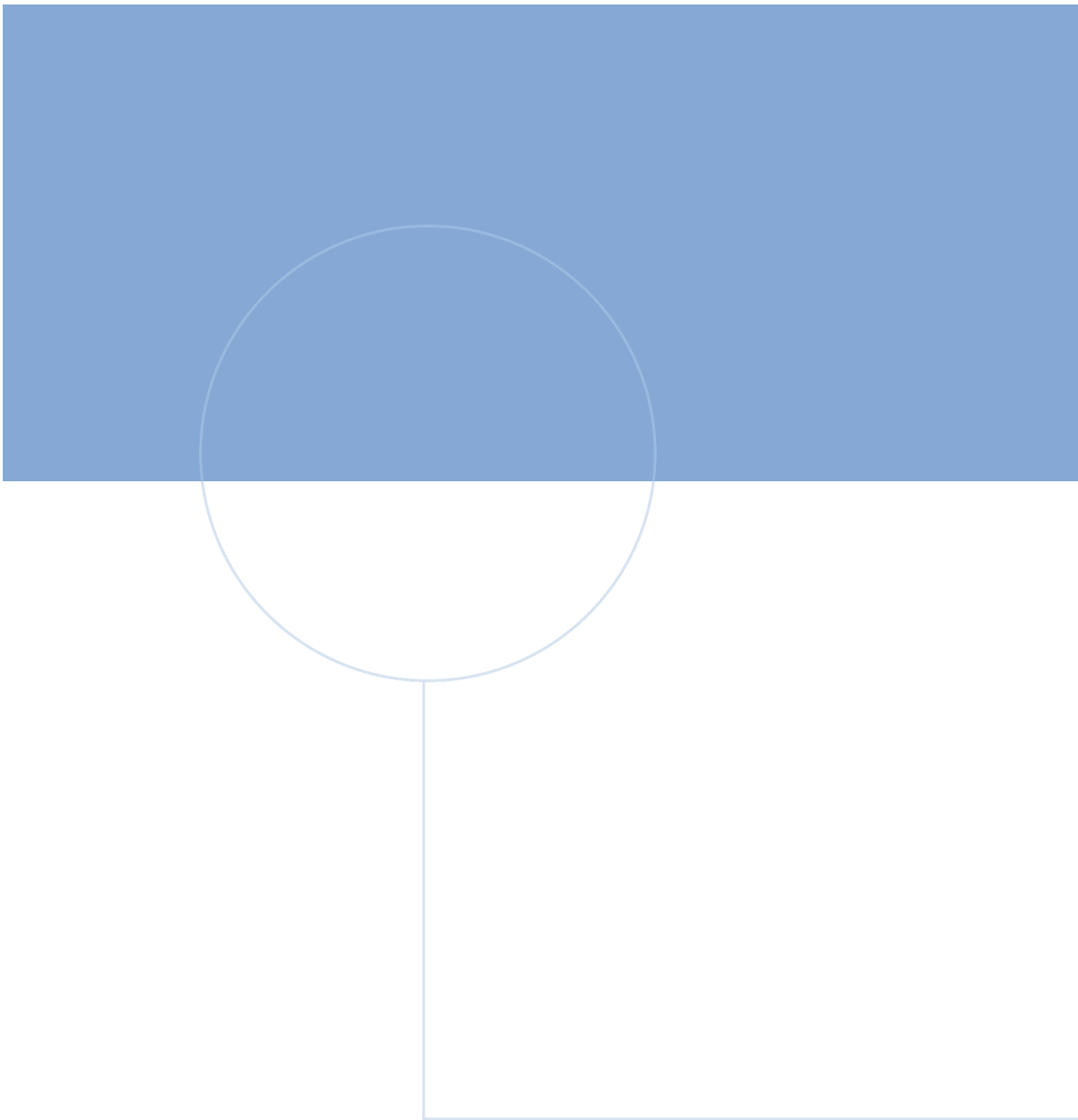

NTNU

Norwegian University of
Science and Technology